Alternative winding wire for induction motor efficiency improvement

Espinoza Audelo Mariana

A Thesis presented for the degree of
Master of Science

Department of Engineering
University of Durham
United Kingdom

December 2021

Dedicated to

My father, my inspiration. This is a dream that came true and it could not be the same without you. I dedicate this to you and I send all my love to heaven for you to celebrate with me. I will be forever thankful for your love and support. Thank you, Dad, for always encouraging me to follow my dreams and pursue my goals, this is for you. I know you will be with me on this journey, forever.

To my mother, my strength, my motivation. Thanks for being my example of passion and effort. I hope one day I become half the woman you are. I dedicate this to you and I thank you for your trust and inspiration to accomplish this life project. I love you.

To my sister, to my brother. Thank you for your support, patience and enthusiasm for sharing this stage with me, You are part of this, never doubt.

To my friends and family, many thanks for all your support, for believing in me and helping me make this happen. This one is for you all.

Declaration

The work in this thesis is based on research carried out in Durham University. No part of this thesis has been submitted elsewhere for any other degree or qualification and it is all my own work unless referenced to the contrary in the text.

Acknowledgements

My endless gratitude to the Consejo Nacional de Ciencia y Tecnologia (CONACyT) and to the Secretaria de Energia (SENER) for their financial support throughout my Master's Degree. Thanks for this opportunity of growing in the professional and personal aspects of life. I would also thank Durham University, Dr. Crabtree and Dr. Donaghy-Spargo for their unconditional support and guidance through my studies.

Alternative winding wire for induction motor efficiency improvement

Espinoza Audelo Mariana

Submitted for the degree of Master in Science
December 2021

Abstract

Of all the electrical energy generated in the world, electric motors are responsible of about 40% of the total consumption and the induction motor is the most popular machine. Focusing on efficiency remains essential to contribute to the energy waste solving. It denotes the utilization of the major amount of electricity and the reduction of the losses in the energy conversion process happening in the induction motor. This losses reduction means savings in both, energy and money, having also a strong environmental impact with the reduction of CO_2 emissions.

This thesis presents a work developed to attempt the stator copper losses reduction in an induction motor. To achieve this, a thermal experiment was designed, where three different insulation arrangements were tested to obtain a temperature rise comparison and with this, obtain and analyse the resistance in function of the temperature. Results demonstrate that the resistance decrease could not be achieved, nevertheless, the experiment and analysis provide a background for further work to be done in order to reduce the stator copper losses with the implementation of a different insulation materials.

Contents

List of Figures

List of Tables

Chapter 1

Introduction

In the recent years, the theme of energy has been growing concerns and interests, both economical and environmental. Greenhouse-gasses emission are having a clear negative impact on climate change and, accurately indicated, the majority of those emissions are due to electricity production [1]. Nowadays, there exist several rotating electrical machines types but induction motors represent the vast majority in the electrical machines market and are responsible for most of the electricity use [2,3]. As mentioned by Wang in [4], an estimate of 7200 TWh of electricity are consumed by electric motors per year, representing between 30-40% of the total electricity consumption [5]. It is necessary to emphasize that this percentage represents electric motors applied in several machine types such as pumps, fans, presses, elevators and centrifugal machines. These are clear examples of essential mechanisms to numerous industrial, transportation, agriculture and commerce processes [6].

Electric motors have primary functional parameters as output power, speed and torque [5]. But also efficiency is a highlighting property, which refers to how well the energy conversion is performed. The term "efficiency" refers directly to the losses in the different parts of the motor during the electromechanical process; reduced losses lead to greater efficiency [7]. Nevertheless, it is impossible to reach 100% of efficiency because energy loss will always be there in its different manifestations as copper losses, core losses, windage and friction.

By studying the losses distribution in an induction motor, it has been inferred that the energy loss in the stator represents the major percentage throughout the

energy conversion process, from the input to the output [7].

Hence, this research is focused on the the stator losses, attempting to decrease them by the implementation of a reduction technique, same that has been selected through a qualitative evaluation, taking into account the loss reducing potential, the feasibility for series production and also the cost rise [8]. Considering the mentioned advantages, the loss reduction technique developed and worked in this research is the implementation of a new insulation material for winding copper wire with the aim of improving heat transfer and reducing winding temperature.

High-efficiency motors offer an increased level of reliability and their maintenance requirements are low, which are important advantages in industry [9]. Energy efficiency started being an important concern in the middle of 1970, when electricity prices started increasing rapidly [10]. That was when motors manufacturers started the energy-efficient motors production. They realized that it was necessary to optimize design, implement higher-quality materials and better electric and magnetic circuits [10]. Contributing to this optimizations and proposing an order to classify motor efficiency, the International Electrotechnical Commission developed IEC 60034-30-1, a standard that classifies electric motors by their nominal efficiency, taking into account the motor power, frequency, number of poles and synchronous speed [11]. Nowadays, the present commercial induction motors efficiency percentages go from 31% to 96.8%, thus, working to improve electric motors efficiency representing a clear opportunity to take in order to reduce energy losses, increase savings in electricity consumption resulting also helpful to reduce energy costs, playing an important role in a sustainable energy future development.

1.1 Research Aims

Recently, numerous works and research have been developed in electric motors in order to improve the energy efficiency of machines. By achieving this improvement, it would be possible to save important amount of electrical energy consumption. Different loss reduction methods as new materials application, new production techniques and cooling improvement have been worked and it has been demonstrated

that the energy saving has been achieved. It clearly represents a huge impact in sustainable future development, therefore, it would be an indispensable requirement to present an economic evaluation, being possible to do calculations to obtain the cost of ownership and the life cycle savings, also obtaining the payback time of the investment to the energy-efficient motor [7].

This research aims at the design and test of a technique with high likelihood to be applied in a stator to support the development of more efficient induction motor. To achieve this, the induction motor will be studied including its variables of speed, resistance and temperature, but focusing specifically on efficiency and losses in order to set the reference for the oncoming changes.

The central purpose of this thesis is to test different stator insulation arrangements and evaluate the performance of a proposed insulated wire. An experimental thermal test will be developed to validate the proposal of the new insulating material, PEEK, which is a thermoplastic owning optimal thermal properties such as excellent thermal conductivity, high operating temperature and chemical resistance [12]. Thermal measurement will be developed in a simulated winding, supplying electric power until thermal steady-state is accomplished. Furthermore, changes in the temperature measurement will be analysed as well as the influence in the resistance value, utilising the obtained temperature data to work out the resistance function in the three different cases. Finally, with the obtained results, it will be possible to define the performance of the proposed insulated wire in the stator winding resistance reduction and be able to suggest the possibility to increase the efficiency of an induction motor by applying the tested changes.

To conclude, with the results obtained, it will be possible to discuss the energy saving potential, the significant reduction on energy consumption and the enormous environmental, technological and economic impact that working on more efficient induction motors may represent for the present and the future of energy.

1.2 Thesis Structure

This thesis comprises 5 chapters including the theoretical and experimental phases of the stator winding simulation in order to compare the resistance rise in winding wires with the application of three different insulation arrangements in order to validate the implementation of the proposed wire to achieve temperature decrease.

Chapter 1 addresses the introduction to energy efficiency in induction motors, providing information of the impact that energy efficiency may have in technical, economical and environmental aspects.

Chapter 2 provides the theoretical background of induction motors, energy efficiency, losses and the existing standards that manage the present induction motor market. An energy economics analysis is also presented where the overall life-cycle cost of the induction motor is evaluated.

Chapter 3 presents the loss reduction techniques to be worked in search of efficiency rise. In this chapter the theory of losses, resistance and temperature is developed, as well as the different types of insulation in induction motor stator winding. The experimental work to be developed will be described here and the system will be fully presented.

Chapter 4 contains the experimental system definition, temperature simulation and the results of the experimental work. Here, the analysis is presented in order to compare and discuss the resulting evidence.

Chapter 5 points out the conclusions and summarises the accomplishments and contributions of this work. Here, future work is also suggested with the possibility of complimenting this research.

Chapter 2

Induction Motor Efficiency

An induction motor is a machine that transforms electrical energy into mechanical energy. It is based upon the application of Faraday's Law and the Lorentz Force on a conductor which explain that when an AC current is supplied to the stator winding it induces an electromagnetic force (EMF) in the rotor, as per Lenz's law, generating then, another set of electromagnets; it is here where the name comes from. The induction motor, shown in Figure 2.1, requires the interaction between the rotating part and the stationary part: rotor and stator. Rotor sits inside the stator with a carefully engineered gap between the two, the air gap [13]. When a 3-phase AC current passes through the stator winding, it produces a rotating magnetic field (RMF) which is the fundamental principle of operation of AC machines. The rotor and the stator are connected by the magnetic field that crosses the air gap; this interaction between magnetic fields generates twist force or torque causes the rotor to turn at a speed that depends on the speed of rotation of the magnetic field [13, 14].

The speed of the magnetic field in revolutions per minute (rpm) is determined by Equation 2.0.1. Synchronous speed is n_s or ω_s, where f stands for the electrical supply frequency (Hz) and p is the number of poles present in the stator.

$$n_s = \frac{120f}{p} \tag{2.0.1}$$

$$\omega_s = \frac{2\pi n_s}{60} = \frac{4\pi f}{p} \tag{2.0.2}$$

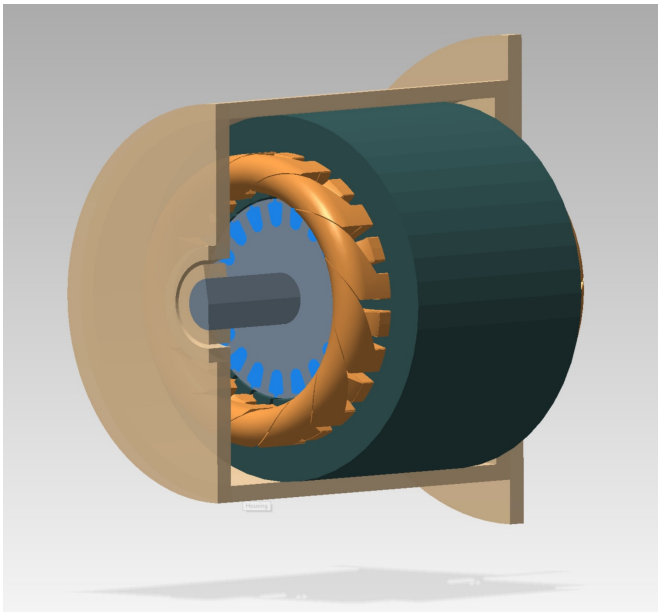

Figure 2.1: Three-phase Induction Motor

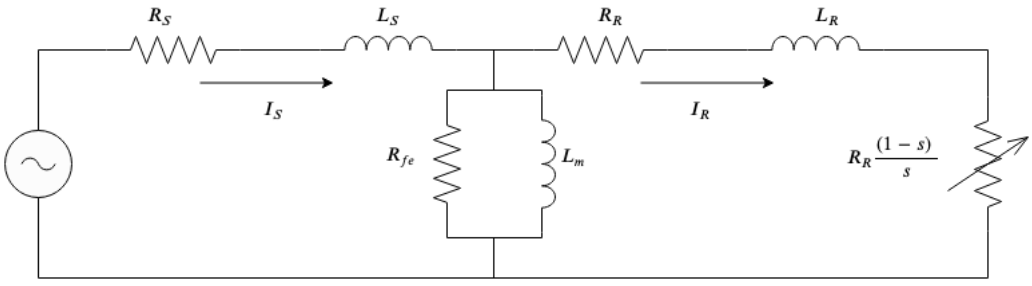

Figure 2.2: Equivalent Circuit of an Induction Motor

In Figure 2.2 the equivalent circuit of an induction motor is presented, where R_s represents the stator resistance, L_s the stator inductance, and I_s the stator current, R_fe is the resistance because of eddy current losses and L_m is the stator magnetizing inductance. Then, R_r is the rotor resistance, L_r is the rotor inductance and $R_R(\frac{1-S}{S})$ is the variable resistance of the rotor. These parameters are the base to determine the input current, speed, efficiency, power factor, starting torque and maximum torque, defining the motor performance as it can be observed in the motor nameplate presented in Figure 2.3 and also by estimating induction motor circuit parameters, motor efficiency under different operation can be evaluated [4].

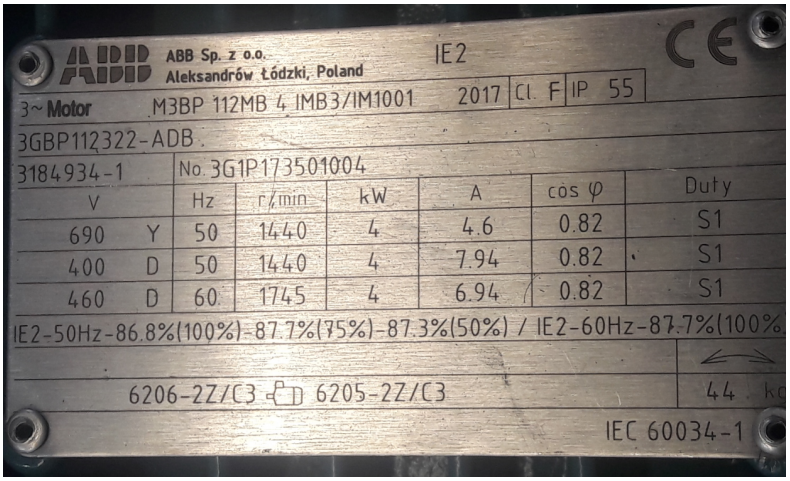

Figure 2.3: Nameplate on an Induction Motor

2.1 Energy Efficiency

Motors are part of the essential machinery in industrial sector as they represent the power, movement and production in the innumerable industrial processes and counting on with motors with high-class performance plays a promising point to focus. In industry, energy conservation and efficiency of machinery have become highly relevant as it contributes in the search of energy and money saving [15]. Thus, replacing standard efficiency class motors for a higher efficient one could have numerous positive economic and environmental changes, for industry and out of the sector and as stated in [5] substantial saving in electricity reductions could lead in the the greenhouse gasses emissions reduction, contributing with this to mitigate the climate change derived of the electricity production [15].

Energy efficiency refers to the real power achieved with the demanded energy and the higher that ratio is, the lower the misspent energy. In an induction motor, efficiency is defined as the ratio of output power to input power, in other words, mechanical output to electrical input, as expressed in Equation 2.1.1

$$\eta = \frac{P_{out}}{P_{in}} \tag{2.1.1}$$

Whenever a machine transforms energy from one form to another, there is always certain loss and results important to analyse and study power losses because it gives a clue as to how they may be reduced [16,17]. Higher efficiency levels lead to lower

losses. In Figure 2.4, a power flow diagram is presented, where the energy loss is typified through the motor process.

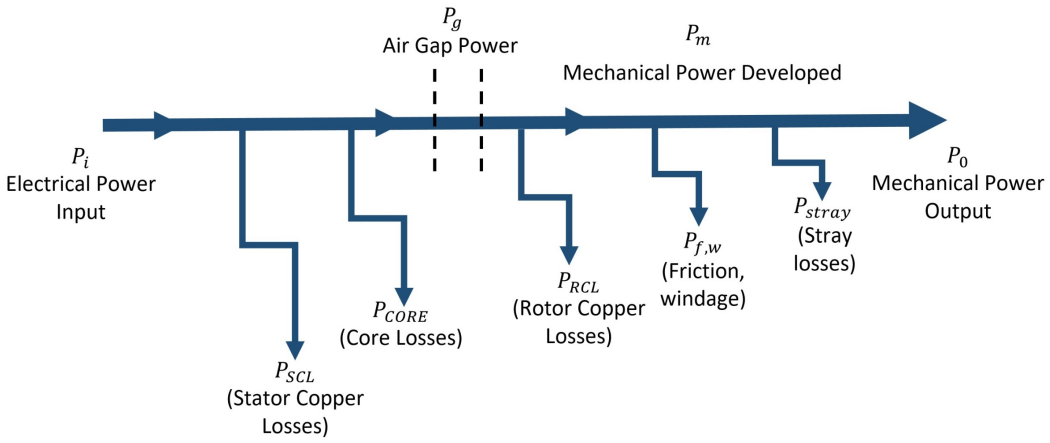

Figure 2.4: Power Flow Diagram

As presented in Figure 2.4, there are five different types of losses [1]:

- Stator copper losses: P_{SCL}, these represent the energy loss produced when the current passes through the stator windings, this generates heat and subsequently, the temperature of the motor rises [18],
- Rotor copper losses: P_{RCL}, these are the losses produced when the current passes through the rotor bars [18],
- Core losses: P_{CORE}, magnetic losses occurred in steel components know as Eddy currents,
- Windage and friction losses: $P_{(f,w)}$, mechanical rotational losses due to the friction and windage,
- Stray load losses: P_{STRAY}, also called additional losses result of the leakage fluxes through the resistance and appear when the motor operates under load.

The efficiency in a motor is also affected by load, rated power and speed: when loads differs from the rated load, there's a negative change in efficiency, on the

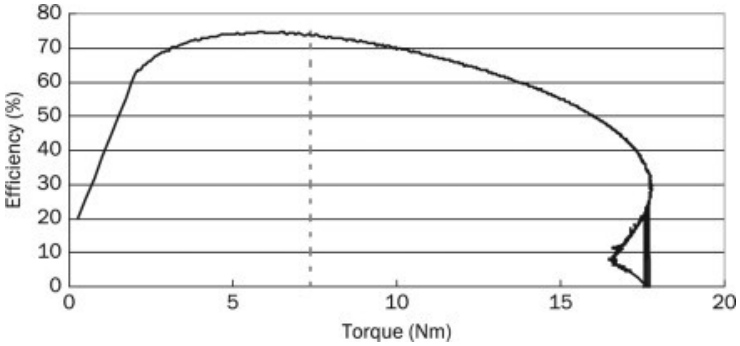

Figure 2.5: Torque vs Motor Efficiency [1]

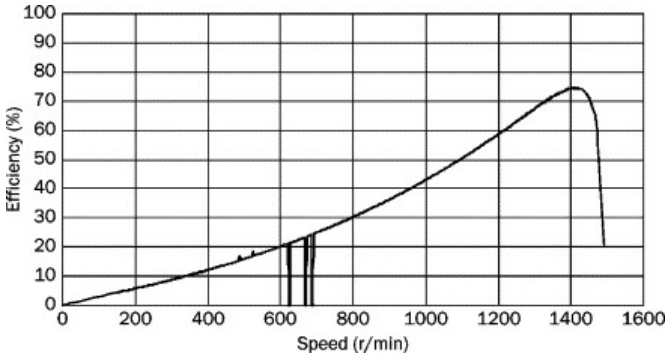

Figure 2.6: Speed vs Motor Efficiency [1]

other hand, efficiency of motors increases with rotation speed until reaching peak efficiency, as it can be appreciated in Figures 2.5 and 2.6 [1].

Another essential factor to emphasize is that the number of poles and the size of the motor affect the efficiency and delimit the importance of the five different types of motor losses, as it can be seen in Figure 2.7. It results interesting to note that in small-medium induction motors, I^2R losses are noticeably dominant. Frequency also affects directly to losses and, as mentioned in [5], the efficiency of 60 Hz induction motors is between 0.5 and 2.5% greater that the efficiency in 50 Hz induction motors, depending of the motor size. Regarding to the output power, it is 20% higher in 60 Hz motors although windage, friction and iron losses increase with frequency [5]. Therefore, most of them develop a better efficiency at 60 Hz compared to that at 50 Hz, becoming easier to reach a higher efficiency when the motor is designed for and operated at 60 Hz instead of at 50 Hz [5].

As mentioned before, calculating the efficiency is mainly related to finding the total losses, thus, it can also be expressed as presented in Equation 2.1.2:

$$\eta = \frac{P_{in} - P_{loss}}{P_{in}} \tag{2.1.2}$$

where P_{in} represents the input power and P_{loss} denotes the overall power losses occurred within the induction motor process.

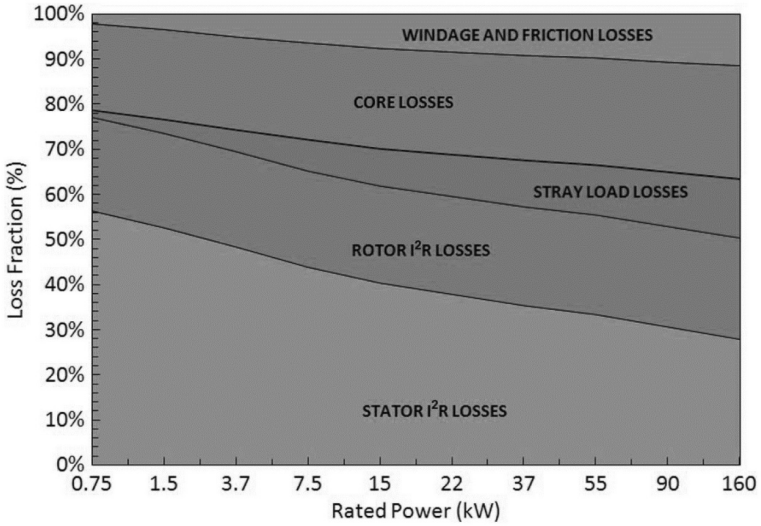

Figure 2.7: Losses as a Function of Rated Power

In Figure 2.7, losses distribution can be appreciated. As it may be observed, stator copper losses dominate the overall power loss, particularly in small and medium sized induction motors [2,10]. Stator copper losses account for 25-55% of the overall losses, rotor losses account for about 20% and core losses account for about 20-25% [19]. These copper losses are also called resistive losses or Joule losses and, as mentioned in [7], they increase proportionally as the temperature rise increases the resistance of the winding. Stator resistive losses per phase are obtained as follows:

$$P_{SCL} = I_S^2 R_S \tag{2.1.3}$$

Where I_S and R_S are the stator current and resistance respectively. The total stator copper losses in an three-phase induction motor will then be:

$$P_{TSCL} = 3I_S^2 R_S \tag{2.1.4}$$

Stray, friction, windage and converter losses are small enough to be negligible, thus Equation(2.1.5) describes the total power losses per phase [20].

$$P_{loss,Total} = {I_s}^2 R_s + {I_r}^2 R_r + \frac{{V_m}^2}{R_c} \tag{2.1.5}$$

Hence, Equation (2.1.2) could be expressed as:

$$\eta = \frac{P_{in} - ({I_s}^2 R_s + {I_r}^2 R_r + \frac{{V_m}^2}{R_c})}{P_{in}} \tag{2.1.6}$$

2.2 Induction Motor Thermal Analysis

During the operation of the induction motor, the heat generated losses (iron losses, stator copper losses and rotor losses), as described in 2.1, affect the efficiency and performance of the induction motor, and these losses can increase the temperature to a limit even larger than the allowable operating temperature, which causes some important problems as presented below [18]:

- Raising the resistance of the stator winding, and consequently increasing the I^2R losses.
- Thermal stresses which may exist in the rotor end rings and bars where most probably a motor breaks down.
- Raising the temperature of stator winding insulation, and subsequently the turn-to-turn or turn-to-ground short-circuit may occur.
- Increasing the temperature rise which has a direct effect on its useful service life [18].

Demanding a rise in the torque or a reduction in the stator frequency can be a significant reason for the current to be increased. This turns out into a temperature rise which means the increasing in stator copper losses and rotor bar losses [21, 22]. As a result of these internal processes, the end winding and rotor bars remain the hottest sections in induction motors [18].

To illustrate temperature rise at the different parts of the induction motor, the lumped-parameter method has been used for a very long time [7]. This model divide the motor geometry due to its different losses and is build based on the main directions of the heat flows. Thus, in this research, stator model is represented by the slot winding and the end windings, including also the stator core. This model is presented in Figure 2.8.

This longitudinal model pictures the cross section of the induction motor stator. The parts are indicated as follows:

1. Stator slot
2. Stator core
3. Left endwinding
4. Right endwinding

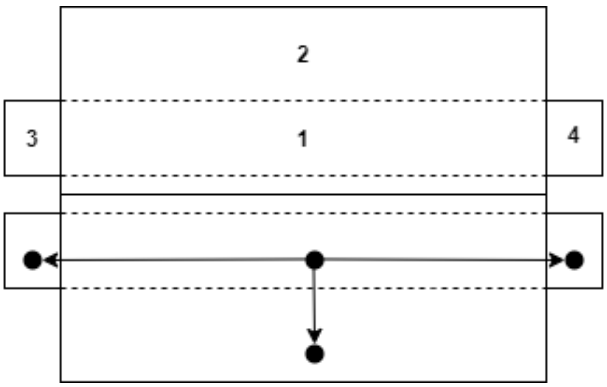

Figure 2.8: Longitudinal Cross Section of Stator

Figure 2.9 is presented to appreciate and comprehend the stator parts in an induction motor.

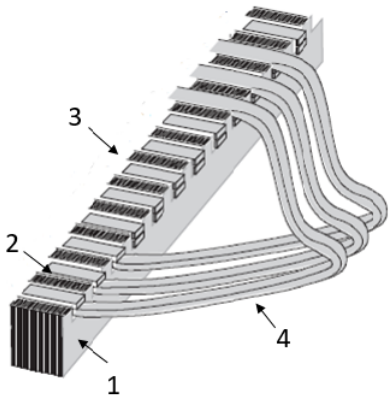

Figure 2.9: Stator Parts

Then, in order to analyze the heat flow and the internal temperatures distribution, a thermal equivalent circuit is developed [23]. Here, each element of the model is represented by a node in the circuit [18]. Resistive losses, iron loses, windage losses and frictional losses are presented by individual heat flow sources and the thermal resistances of iron cores, insulation and the frame are given as resistances [24]. Pyrhonen presents in [7] a thermal equivalent circuit of a typical electrical machine. It can be observed in Figure 2.10

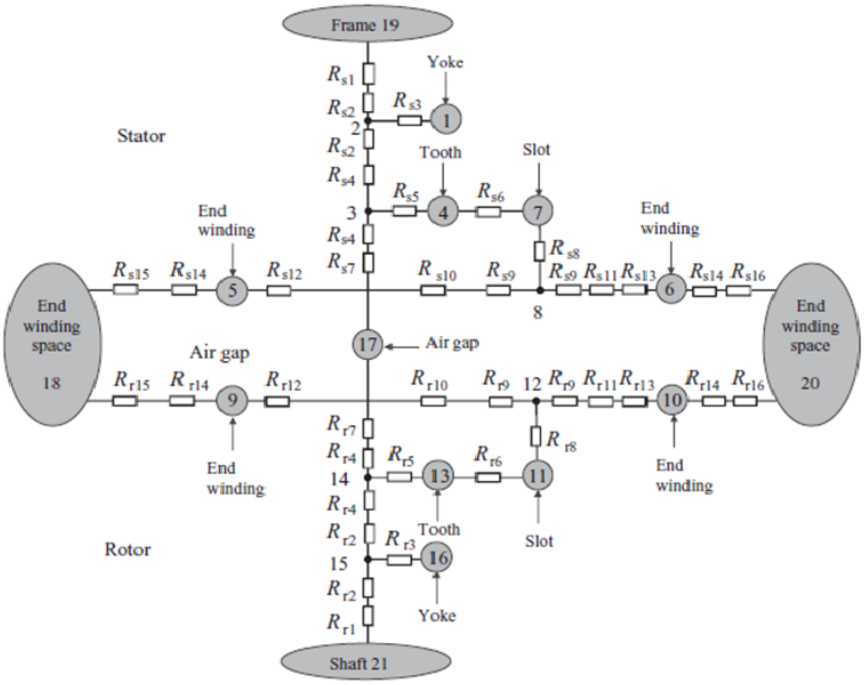

Figure 2.10: Electrical machine thermal model

Based on this, Figure 2.11 represents the stator thermal equivalent circuit analyzed in this thesis, where the nodes represent the heat sources generated in the stator due to the losses. As mentioned in [25], in each node of the circuit the thermal capacitance of each element is implicit, and, $R1 - R6$ represent the thermal resistances which are connected between each two neighbouring nodes. This thermal resistance impedes the heat transfer from one component through the other.

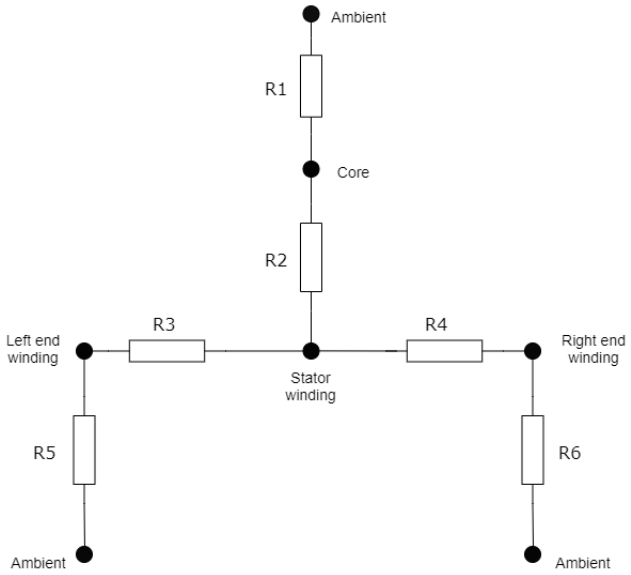

Figure 2.11: Thermal Equivalent Circuit

The components on this circuit keep their properties as constant, since the only element to be analyzed in the experiment are the windings and their different insulation characteristics. Resistances stated in this circuit are the only element to be analyzed in the experimental section of this thesis.

2.3 Efficiency Standards

Global electricity consumption is boosting as technology is being developed. Therefore, it turns essential to increase efficiency of the used energy. Standards of electric motors have the purpose of attempting to specify the performance in the industry of three-phase induction motor, which constitute the large majority of motors over 0.75kW, and, consequently, are responsible for most of the motor electricity consumption [26]. Some of those standards will be presented in the chapter.

Standards aim to achieve the harmonization of the different requirements for induction motors efficiency levels around the world, including efficiency testing and classification and they remain essential to support successfully a global motor market transformation, meaning a strong impact on the electrical energy consumption in the world, mainly in fast developing countries [5].

Motor efficiency levels started to grow in the early 1980's and there were not standards for efficiency levels. Nowadays, there exist many different energy efficiency standards for induction motors. The first cited example is the Energy Policy Act in USA (EPAct) which dictates that three phase motors between 1-200 HP must obey NEMA MG-1 standard [27]. National Electrical Manufacturers Association (USA) started to define energy efficient levels on the early 90's and by 2001 the first NEMA premium efficiency standard was established. The European Committee of Normalisation in Europe, Canadian Standards Association establishes motors regulations in Canada, Japanese Industrial Standards in Japan, Guobiao in China and also several regulations that are being developed attempting to cover general characteristics such as duty and rating, service and operating conditions, limits of temperature rise, vibration, dimension, noise levels, enclosure, methods of cooling and efficiency [13].

Nevertheless, it resulted really complicated for the induction motor manufacturers to cover the global market and satisfy regulations and laws all over the world. For these reasons, the International Electrotechnical Commission, whose objective is to promote international cooperation on all questions concerning standardization in the electrical, electronic and associated fields, developed in November 2008 the IEC 60034 in order to harmonize the differences and create a competitive electric motor

transformation, integrating 0.75-70 kW motors, including different supplied voltages and frequencies [4, 5]. After that, Standard IEC 60034-30-1 included specification of the classes for fixed- and variable-speed electric motors that have a rated output from 0.12 kW to 800 kW.

The class designation defined by IEC consists of the letters "IE" as short for "International Energy Efficiency Class" and followed directly by a number, 1-4, representing the classification. Standard IEC 60034-30-1 developed a full classification of motor rated from 2, 4, 6 or 8 poles and 50Hz or 60 Hz presenting tables with nominal efficiency limits percentage for classes IE1, IE2, IE3 and IE4 as it can be observed in Figure 2.12. This graph was produced to illustrate the data presented in Standard IEC 60034-30-1.

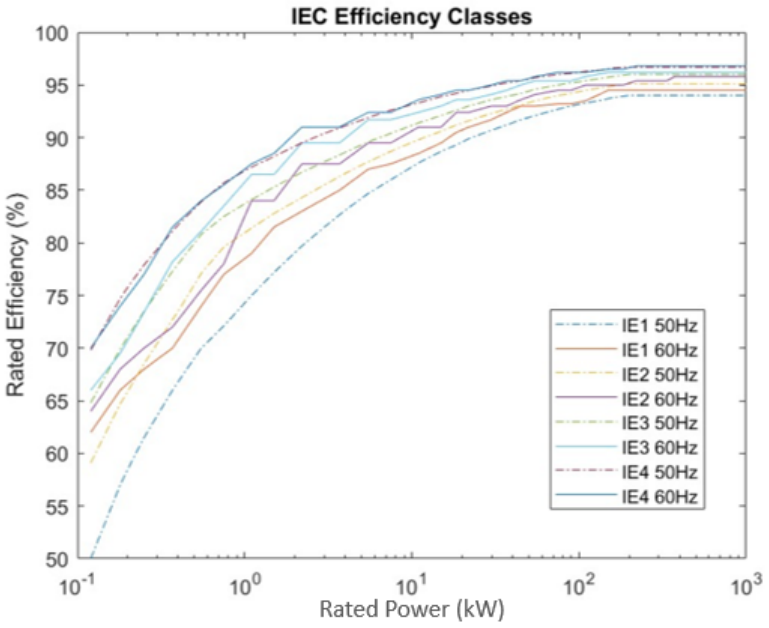

Figure 2.12: IEC Efficiency Classes

The nominal limits of efficiency classes are fully presented in IEC 60034-30-1:2014. Standard 60034-2-1 also establishes the methods for determining losses and efficiency from tests applying to induction machines of all sizes within the scope of IEC 60034-1.

After the implementation of IEC standards, the rated efficiency and IE class must be clearly indicated on the motor rating plate, specified next to the frequency

rating as there are motor working with both, 50 Hz and 60 Hz as presented on Figure 2.12 [5].

The existing induction motor market, principally in developed countries, is currently moving towards classes IE3 and IE4 as a result of the global effort of working in the use of efficient products reduction of energy consumption and CO_2 emissions [9,27]. For these reason, establishing minimum energy performance standards (MEPS) is a powerful tool to force electric motor market to that needed transformation [5]. Nowadays, the governments establish their minimum efficiency performance standards in every country based on IEC standards; IE3 is mandatory in the USA since 2011, IE2 in China since 2011 and IE3 in the European Union countries since 2015 [2]. Nevertheless, they could be changing as higher efficiency classes are being introduced [28].

Enforced regulations are being adopted worldwide to accelerate the motor market transformation toward Premium/IE3 and Super Premium/IE4 efficiency classes [9]. Minimum energy performance standards seem also essential to remove inefficient motors from the market and to support energy-efficient models which are actually cost-effective on a life-cycle basis [5]. Table 2.1 summarizes IEC efficiency classes.

Class	Name
IE1	Standard Efficiency
IE2	High Efficiency
IE3	Premium Efficiency
IE4	Super-Premium Efficiency
IE5	Ultra-Premium Efficiency

Table 2.1: IE Code

Currently, class IE5 has been introduced, but, as presented in [5], there is not sufficient market and technological information available to establish neither a mandatory IE4 standardization. However, the levels of the IE5 efficiency class whose goal is to reduce the losses by 20% relative to IE4 are predicted to be incorporated into the next edition of the IEC 60034-30 standard [28].

Even though a higher efficiency induction motor means a higher investment, they

offer an increased level of reliability. As Ferreira indicates on [7], higher efficiency motor offers numerous benefits on life expectancy, lower harmonic losses and tolerance to voltage unbalance. These motors also reduce maintenance requirements and several economic advantages compared with standards motors and, as specified in [27], high efficient motors can pay for they additional cost within 2-4 years.

In these days, it is plenty difficult for manufactures to reach high efficiencies levels without doing electrical redesign or using larger frame sizes [27]. Thus, several research and tests are being made, developing new techniques and testing diffe-rent materials taking into consideration the substantial potential for saving energy and money by working on motors efficiency improving.

2.4 Energy Economics

Near 30 million new electric motors are sold each year for industrial application and around 50 percent of all electric motors are operated in USA, EU and China [1]. Electric motor sales grows as economies do and it has been demonstrated that those sales increases 10% by year [29]. The question is if the additional manufacturing cost is covered by the efficiency gain for a given rated power, number of operating hours, load factor, and electricity cost [2].

Therefore, improvements in the energy-efficiency of electric motors can contribute to improve savings in terms of energy, carbon dioxide emissions and money. Even though the major market remains IE2 and IE3 motor, main researchers find feasible to propose IE4 and IE5 efficiency class motor as mandatory to start mass production [8,19]. Moreover, including efficiency testing and classification, seem essential to promote effectively a global motor market transformation, which will have a strong impact on the electrical energy consumption all over the world, particularly in fast developing countries as China, USA and EU [5].

Even though, producing high-efficiency induction motors result more expense than standard ones, several studies have demonstrated that the electricity consumption leads to short paybacks periods on this kind of investment [23]. The use-phase cost of most electric industrial motors, including the consumed energy

and maintenance costs, dominates by far their overall life-cycle cost (LCC) [5].

Minimizing the losses is the main purpose of energy efficiency improvement. By increasing efficiency and implementing more efficient motors, it would be possible to reach huge saving in both energy and carbon dioxide emissions. Implementing higher efficiency electric motors can lead also to significant reductions in the energy consumption and also reduce the environmental impact, therefore, it remains critical to promote the replacement of old inefficient motors to more efficient ones [5].

It is known that power is the flow of energy, hence, its cost should be measured in money (£) per hour [30]:

$$C_e = \frac{£/h}{W} = \frac{£}{Wh} \tag{2.4.1}$$

To obtain a payback time of the investment to an energy efficient motor it is necessary to calculate first the savings C_s per year[10]:

$$C_s = C_e P_{diff} T \tag{2.4.2}$$

where P_{diff} is the reduction of the motor losses. Thus, the saving per year may also be expressed as follows:

$$C_s = C_e P_{out} \left(\frac{1}{n_1} - \frac{1}{n_2} \right) T \tag{2.4.3}$$

where P_{out} is the power output of the compared motors and n_1 and n_2 are the efficiency values.

As mentioned before, there is an increase on the investment by purchasing a more efficient motor. That difference will be denoted as C_{diff} to calculate the payback time T_{pb}:

$$T_{pb} = \frac{C_{diff}}{C_s} \tag{2.4.4}$$

As revised, focusing on purchasing and consumption is no longer sufficient due to factors that affects the induction motor total costs. To make a further study and evaluate the economic performances of the product during its entire life, a total Cost of Ownership must be obtained.

The total cost of ownership of an electric motor integrates the cost of purchase price which variates according to the class, the cost of running and the cost of not running. The consumed electrical energy, dominates by far their overall life-cycle cost due to the cost of running represent the longer period on a motor life. Depending on the cost of electricity, a more efficient motor can pay for its additional cost over the energy efficient motor within 2-4 years [27]. The Cost of Ownership of an electrical motor can be expressed as follows [29]:

$$COO = P_p + C_r + C_{nr} \tag{2.4.5}$$

Where P_p is the purchase price, C_r stands for costs of running and C_nr is the cost of not running.

The cost of running are obtained by:

$$C_r = P_{in} C_e T_r T_t \tag{2.4.6}$$

Where P_{in} represents the input power in W, C_e is the cost of energy in £$/Wh$, T_r is the running time in hours and T_t the motor lifetime in hours.

In addition, the costs of not running are defined by the unplanned downtime in the production each year. They may be estimated by:

$$C_{nr} = C_f T_d \tag{2.4.7}$$

Where C_f stands for the failures cost per hour and T_d is the downtime in hours.

It is noteworthy that the purchase price represents only around 3% , whereas the running costs represents between 70% and 95%. Moreover, the cost of not running remain around 2-30%. Thus, when purchasing an induction motor, running and not running costs should be considered in addition to the purchase price as they have a significant impact on the total cost of ownership [29]. In addition to these data, the potential life cycle of the purchase can also be analysed by calculating the effect of the cost of money over the lifetime of the motor, thus, considering the "present worth factor of an equal payment series" as

$$k_{pw} = \frac{(1+i)^n - 1}{i(1+i)^n} \tag{2.4.8}$$

Where i is annual interest and n the years of motor lifetime. Thus, the present value of the cost of 1kW of loss over the motor life C_{pw} is

$$C_{pw} = k_{pw} C_e T \tag{2.4.9}$$

In [31], an evaluation of IE3 and IE4 classes has been developed. In this study, 75 kW, 4 pole induction motors were tested for a fixed-speed pump unit application. It concluded that the IE4 motor is more profitable than the IE3 motors when the operation time is more than 3 years, due to the initial investment which is higher in the IE4 motor. The payback time obtained for the IE3 motor was 5.2 years and for IE4 motor was 2.9 years.

Performing this type of economical evaluation can deliver results of how reliable is investing in higher efficiency induction motors, considering not only technical characteristics but including also costs of energy, running and costs of ownership, savings and payback time, being these key concepts for industries to decide to make an investment.

Chapter 3

Loss Reduction Techniques

Energy conservation is an important issue regarding to the increase of environmental problems in the recent years. Induction motors have the potential of contributing to a carbon dioxide emissions drop if an improvement in design is developed. As mentioned in Chapter 2, the stator is the location where the highest percentage of losses are presented and these remain the major energy losses in an induction motor and also different types of electrical machines [32]. Therefore, the technique investigated in this thesis attempts to demonstrate power efficiency gains by implementing changes in the stator, I^2R, or stator copper losses, with a view that these can be successfully reduced and higher efficiency is achieved.

In this section, fundamental background is presented to conceptualize the methodology to be worked in this research. As explained in Chapter 2, there exist different possibilities and techniques that can help to decrease the different type of losses in induction motors. Different loss reduction methods were consulted and considered, and according to [8] they could be classified as below:

- New materials
- New production techniques
- Improved cooling

Motor manufacturers usually use more materials such as magnet wire and electrical steel to improve efficiency. But using more material means increases the motor

cost and meanwhile will increase the motor physical size [6]. In [33] Cheol-Ho and Tae-Uk Jung investigated a concentrated winding method in order to reduce the material use and consequently the cost of the induction motor. They mention that the coil length and resistance may be reduced, nevertheless with this method, increased harmonic losses and torque deterioration may occurred.

In [17] Preecha and Dejvises calculated the losses in electrical machines considering and measuring the ventilation wind temperature developing a technique where efficiency and power losses can be determined with no need of stopping operations. Moreover, in [34] an evaluation of two different types of winding fill factor was developed to compare thermal conductivity, where infiltrated winding, technique where windings are impregnated or varnished in order to reduce the unwanted air leaks into them and the non-infiltrated winding, the ones that are not impregnated, were compared. Meanwhile, in [32], concentrated and distributed winding were evaluated to compare the performances and prove the impact that the winding configuration has in the torque and harmonics. Likewise, a thermal improvement technique was developed by Galea and Gerada, where the insertion of a low-resistance heat path attempted to improve the temperature distribution in the slots [35]. A different technique is explained in [36], where different technologies are discussed in order to achieve the maximum fill factor. This refers to the amount of copper that can be placed in a slot, as it can be appreciated in Figure 3.1 where the orange section represents the copper filling completely the slots and the color green represents the stator core. A direct consequence of a higher fill factor is the amount of air in the slot, this is significantly reduced and replaced by copper. The fill factor should be as high as possible as it influences the machine efficiency and performance [37].

Makita and Ito also attempted for a technique taking into account the fill factor method, proposing a new motor with high winding factor and high slot fill factor manufactured by mounting distributed windings in a flat stator core, joining opposite ends of the bent stator together [37] where a rated efficiency of 76% could be obtained with an alternative motor model . The same way, in [38], Di Tommaso and Genduso developed an algorithm to performe the calculation of fill factors. Similar to them, Herrman and Stenzel also worked the fill factor and the slot geometry creating four

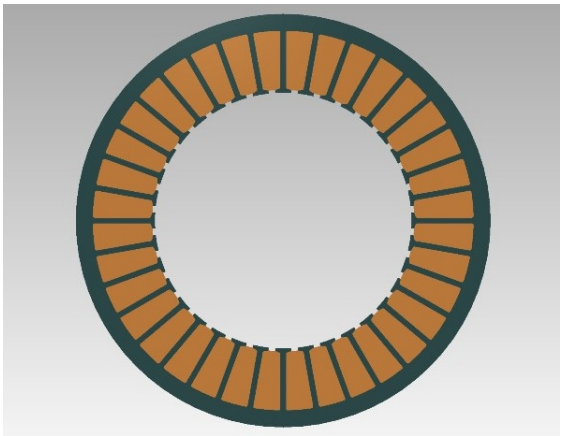

Figure 3.1: Stator Winding Fill Factor

optimization algorithms to obtain the exact wire placement trying to achieve the maximum fill factor in stator slots [39]. In [40], it is explained how Sang-Bin Lee and Thomas G. Habetler worked in the stator resistance monitoring to obtain and evaluate the temperature rise in the stator. The method executed in [41] performed a thermal analysis of the motor winding based on mathematical circuit modelling, where the real behaviour of the machine in operation can be reflected. Alternatively, in [42] a resistance estimation technique was applied in an induction motor stator winding where a DC injection method was used for temperature monitoring.

As presented here, several techniques have been investigated in an attempt to reduce the stator copper losses and with this, achieving the pursued efficiency increment. After a wide background was consulted, a qualitative and quantitative evaluation taking into account the loss reduction potential, feasibility for mass production and cost rise, it was possible to design and establish the method to be applied: the implementation of PEEK insulated coper wire in stator winding, which will be described in the next sections.

3.1 Influence of Insulation Materials

The fundamental components in a stator are the copper conductor, the stator core and the insulation [43]. The copper conductor is the conduit for the stator winding current and it is critical it to have a cross section large enough to transmit all the

current required without overheating [43]. The stator core concentrates the magnetic field on the copper conductors in the coils and the final major component of a stator winding is the electrical insulation. As presented in [7] the insulation systems in electrical machines comprises distances and insulator materials, which are defined as nonconductive materials. Insulation is essential as without it, copper conductors would come in contact with one another or with the grounded stator core, causing the current to flow in undesired paths and preventing the proper operation of the machine. In addition, indirectly cooled machines require the insulation to be a thermal conductor, so that the copper conductors do not overheat. Moreover, the stator winding insulation system contains several different features, which together ensure that electrical shorts do not occur, the heat from the conductor, I^2R loss, is transmitted to a heat sink and that the conductors do not vibrate notwithstanding the magnetic forces [43]. According to Joule's law, the energy consumed by resistance is converted into heat [44]. If the operating temperature is lower, the I^2R will also be, due to the stator circuit resistance, contributing to decreasing heat losses and consequently the efficiency increase.

On the other hand it is worth to mention that motor designers would consider ideal to eliminate the electrical insulation, as the insulation increases machine size and cost, without helping to create torque or current. Unfortunately it is not currently possible, therefore insulation system is a significant field to study and improve.

Studying the winding wire it can be stated that is composed of two parts, the copper conductor and the insulating layer. When the wire is electrified, its outer surface is the one that contacts with low temperature atmosphere and its interior is high temperature electrified copper conductor [44]. In Figure 3.2 a wire cross section can be appreciated, where r_1 denotes the copper wire and r_2 includes the insulation layer.

Temperature rise in the stator winding is caused by power loss inside the machine in which the main contribution comes from the current flowing through the stator winding [45]. To develop thermal management in electric machines and maintain temperature control, there exist different insulation methods and materials that can minimize losses, particularly copper losses, and yield improved performance,

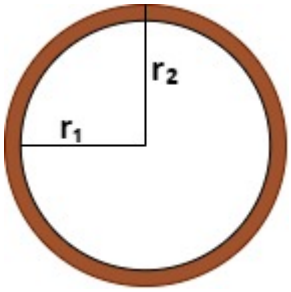

Figure 3.2: Wire Cross-section

reliability and efficiency.

Insulation is achieved due to a nonconducting material with a low conductivity improving also the winding structures [7]. The most common insulating materials are mica, polyester or epoxy resins, aramid paper and polyester films.

The maximum operating temperatures of those materials depends completely on the insulation thermal classes and, according to IEC 60085, insulation materials are classified according to their ability to resist high temperatures without failures and is important it to be higher than the hottest spot of the stator winding [9]. As presented on [7, 46], the most common thermal class in electrical machines is F (155) where the thermal class represents the hot spot allowance. Table 3.1 shows the thermal classes according to IEC 60085 [47].

Thermal Class	Letter Designation
90	Y
105	A
120	E
130	B
155	F
180	H
200	N
220	R
150	-

Table 3.1: Thermal Classes of Insulating Materials

As indicated in [45], the stator integrity is primarily related to the insulation system. The most challenging task in an electrical machine insulation construction is the insulation of conductors and it is also the thinnest insulation component [9]. This type of insulation is often a varnish-like thermoplastic; wires are coated with repeated layers, often using 2 different materials to achieve better thermal resistance, better mechanical properties and improved cost efficiency [7].

In this thesis the proposed insulator material is PEEK (polyether-ether ketone), which represents an alternative to use a single material, as this is a very good heat conductor insulator. It is a semi crystalline, high-temperature engineering thermoplastic, owning an operating temperature of up to $260°C$ that is excellent for applications where thermal, chemical, and combustion properties are critical to performance [48] as it owns a owning a good thermal conductivity. PEEK insulated wire owns key properties to perform in challenging industrial environments and it is applied in electric motors, generators, transformers and solenoids in automotive, aerospace and electrical industries [49, 50]. PEEK mechanical and electrical characteristics are presented in Table 3.2 comparing it with Polyurethane insulator.

Characteristic	Unit	PEEK	Polyurethane
Tensile strength	MPa	95	64.5
Elongation at break	%	25	26.8
Flexural modulus	MPa	3800	2280
Modulus of elasticity	MPa	3650	2580
Density	$\frac{G}{cm^3}$	1.31	1.45
Continuous operation temperature	$^\circ C$	250	155
Dielectric constant		3.5	-
Dielectric strength	$\frac{kV}{mm}$	23	15.7
Dielectric dissipation factor		0.004	-
Melting point	$^\circ C$	334	218
Moisture absorbency	% by weight	0.5	0.238
Resistivity	Ω cm	$1.0\text{x}10^{16}$	$0.075\text{x}10^{16}$
Thermal conductivity	$\frac{W}{mK}$	0.25	0.022
Specific heat capacity	$\frac{kJ}{Kg^\circ K}$	0.32	0.0012

Table 3.2: Insulators Characteristics

3.2 Effect of Temperature on Resistance

The temperature rise in induction motors is considerably reduced in Premium (IE3) and Super Premium (IE4) classes due to the lower losses and improved heat dissipation [9]. In an induction motor there are three different mechanisms that dissipate heat energy as a result of losses: conduction, convection and radiation. Considering the stator losses, convection is the mechanism that transfers the heat from inside the coil, the solid medium, to the ambient, the surrounding fluid [51]. The power loss in the form of heat generation caused by the electric current circulation is defined as Joule effect [52]. Whenever a current passes through a conductor, there will be a change in the temperature, this is due to the lost energy which is converted into heat. As Cengel mentions in [51], heat is generated in the wire and its temperature rises as a result of resistance heating. The resistivity of a material, defined as the ratio of the magnitudes of electrical field and current density, varies with tempera-

ture, thus, resistance of the material will also varies as it can be deduced with the resistance function [52]:

$$R = \frac{\rho L}{A} \tag{3.2.1}$$

where ρ is the resistivity of the conductor material, L is the length of conductor and A is the cross-sectional area of conductor. It is essential to mention that if ρ remains constant, then so is R, when L and A do not change [52]. However, as stated before, resistivity varies with temperature. This variation is represented by equation 3.2.2 where temperature dependence of resistivity is defined:

$$\rho = \rho_0[1 + \alpha(T - T_0)] \tag{3.2.2}$$

where ρ_0 is the resistivity corresponding to T_0, this is the reference temperature often taken as 0°C or 20°C, where the resistivity value is 1.72x10^{-8} and T is the subsequent temperature that can be either higher or lower than T_0. The temperature coefficient of resistivity is represented by α, and as appreciated in Table 3.3, it is different for every conductor [52].

Material	$\alpha(°C^{-1})$
Aluminium	0.0039
Brass	0.0020
Carbon	-0.0005
Copper	0.00393
Iron	0.0050
Lead	0.0043
Mercury	0.00088
Silver	0.0038
Tungsten	0.0045

Table 3.3: Temperature Coefficients of Resistivity

As it can be clearly observed in Equation 3.2.1, the resistance increase in a conductor of uniform length and cross section, corresponds to increasing the resistivity.

Thus, the resistance variation is linear to resistivity. The same way in Equation 3.2.2, where resistivity is linear to the temperature change. This way, resistance function can be expressed as follows:

$$R = R_0[1 + \alpha(T - T_0)] \tag{3.2.3}$$

This will be then the function to be used in the experimental work developed in Chapter 4, where the influence of the temperature in the resistance of a stator winding model is studied and analysed.

Chapter 4

Experimental Work

4.1 Experimental System

The temperature rise affects highly on the maximum output power of electrical machines. Therefore, heat transfer design is as important as electromagnetic design. According to this fact, a temperature-based resistance estimation represents an effective way to calculate copper losses in stator winding. To begin with the experiment modelling, the first features to consider are the wire characteristics. As specified in 3.1, the winding wires have the insulation component. Copper wires are coated with insulator materials according to the thermal classes. For thermal class F (155), the materials used to cover copper wires are inorganic materials as mica, parylene, polyurethane, glass fibers, PTFE and asbestos. The thermal conductivity of these materials are between 0.11-0.22 $\frac{W}{mK}$. PEEK has a thermal conductivity of 0.25 $\frac{W}{mK}$ [7]. To illustrate the behaviour of the wires, these were simulated with COMSOL Multuphysics to determine the temperature rise of both models. In this test, a wire section of 1 meter was simulated as reference for the experiment. The parameters considered for the simulation in COMSOL Multyphysics are summarized in Table 4.1. These parameters were introduced in the settings of Heat Transfer Module in the software for it to run the simulation in order to measure the temperatures rises. Temperatures results are presented in Table 4.2.

Variables	Varnish Insulated Wire	PEEK Insulated wire
Wire Length	1 m	1 m
Surrounding Temperature	20°C	20°C
Thermal Conductivity	0.22 $\frac{W}{mK}$	0.25 $\frac{W}{mK}$
Current	6 A	6 A
Copper Diameter	1.22 mm	1.13 mm
Insulator Width	0.07 mm	0.12 mm

Table 4.1: Parameters for Simulation

In Figure 4.1 the cross-section of the wires in simulation are shown. Here, the differences in copper wire width and the insulator width can also be observed.

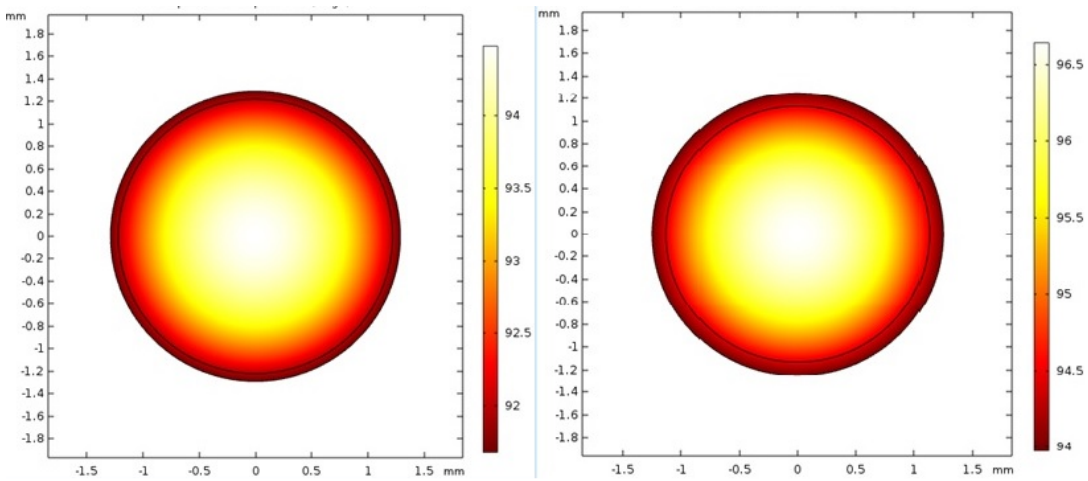

A. Varnish Insulated Wire B. PEEK Insulated Wire

Figure 4.1: Temperatures Comparison

Wire	Minumum Temperature	Maximun Temperature
Varnished Insulated Wire	91.5°C	94°C
PEEK Insulated Wire	94°C	96.5°C

Table 4.2: Temperatures in Simulation

The development of the thermal experiment in this research was based on the induction motor stator model, which is composed by the core and the winding, same that can be appreciated in Figure 4.2. This method is non-invasive to the windings and it can be applied in any operating electrical machine.

Figure 4.2: Stator Core

In figure 4.3, the stator core is illustrated. Here, it can be observed that it contains slots where the winding is built.

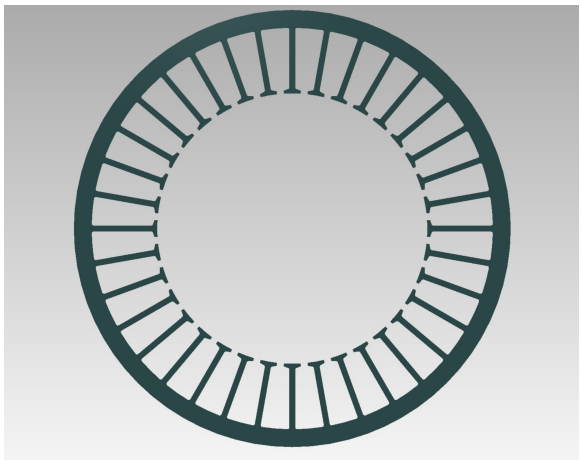

Figure 4.3: Stator Core

The proposed experimental model attempts to simulate a small section of the stator core, consisting of 2 slots to create the coil, as shown in Figure 4.4, where

A is the base and B is the model top. Both pieces are assembled as presented in Figure 4.5.

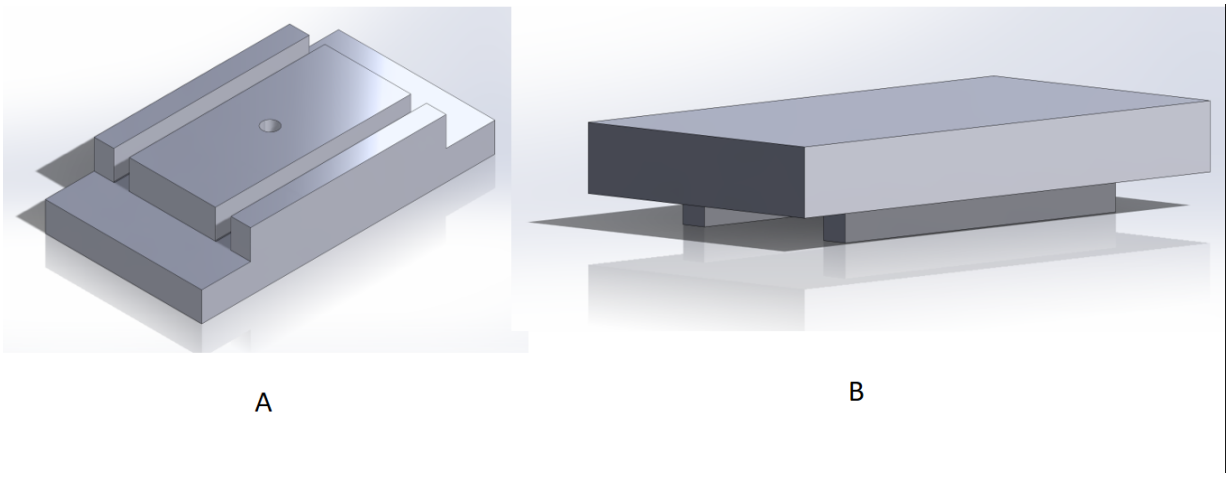

Figure 4.4: Stator Base and Top

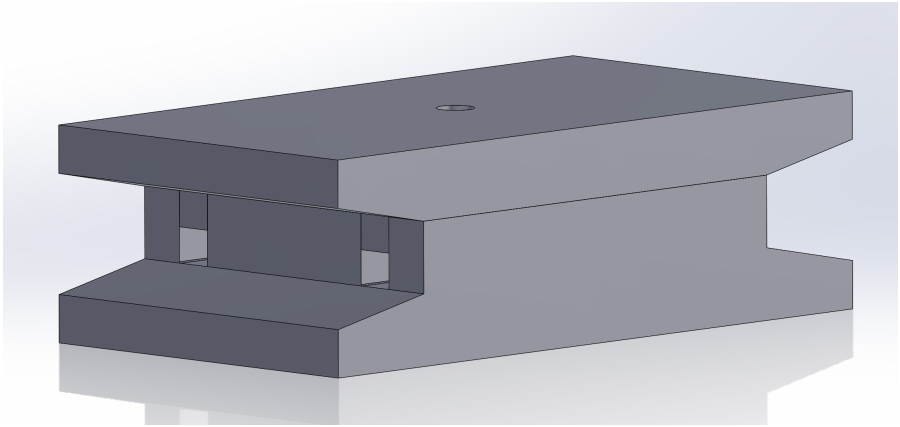

Figure 4.5: Stator Assembly

The objective of the experiment is to test the three different insulation arrangements aiming to compare the temperature rise. However, the focus is to verify PEEK feasibility and performance and how it can influence induction motor efficiency by decreasing the temperature in the stator winding.

Due to the restrictions of the materials, it was decided to create a small experimental section in order to use just a small amount of PEEK insulated wire to run the corresponding tests. To obtain the stator section model, it was necessary to work with Solidworks and create the mechanical model. The obtained Computer Aid Design was taken to the mechanical workshop for it to be manufactured and then, proceed to create the winding manually. The model dimensions are presented in Table 4.3.

Magnitude	Value
Length	150mm
Width	80mm
Base Height	30mm
Slot width	8mm
Slot depth	15mm
Top Height	22.5mm
Top bars height	7.5mm

Table 4.3: Model Dimensions

The slot cross area to be filled with the wire was then $60mm^2$. Hence, a 30 turns coil packing patter was chosen to be created in the slots because of its ease to be wound manually, as shown in Figure 4.6.

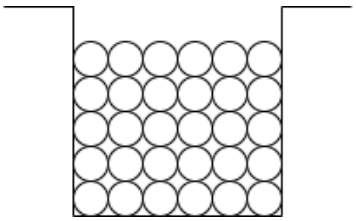

Figure 4.6: Stator Slot Cross Section

Once the experimental coil was defined, a fixed current and reading time intervals were established. The variables of the created system is summarized in Table 4.4.

Variables	Value
Coil length	8.7 m
Coil turns	30
Sampling Time	15 min
Current	6 Amps

Table 4.4: System Conditions

These conditions were the same to create the three windings. The distinctive was only the insulation arrangements to be compared. These are listed below:

1. Varnish insulated copper wire
2. Varnish insulated copper wire and slot liner
3. PEEK insulated copper wire

The model can be observed in Figure 4.7.

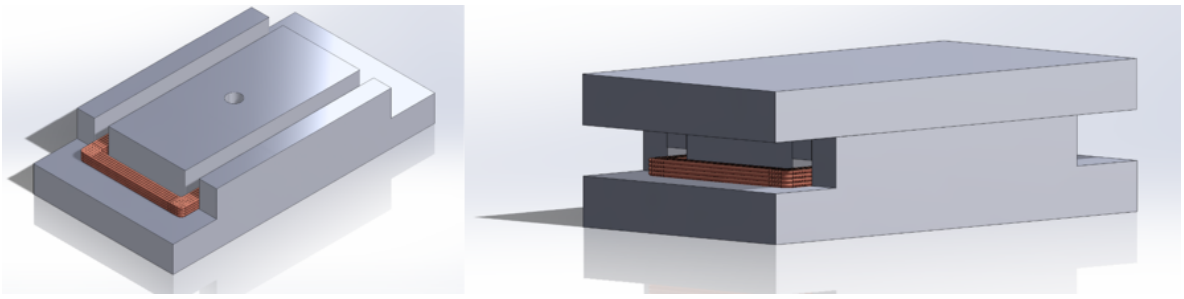

Figure 4.7: Winding Model

In order to measure the temperature, Picoscope TC-08 was the instrument used to obtain the temperature information. This is a 15-channel programmable data logger that links the sensor and the software interface used to observe the readings. This software was PicoLog 6. It offers the possibility to export the temperature plots and also de data as *.csv* files. PicoLog 6 interface is shown in Figure 4.8.

Figure 4.8: PicoLog 6 Interface

It can be observed that this interface contains channels, same that corresponds to ports in the Picoscope. The sensor used to read the temperature for every channel was a Thermocouple type K. These devices can be appreciated in Figure 4.9.

Figure 4.9: Picoscope TC-08 and Thermocouple Type K

Once the model was ready, the thermocouples were placed in key spots. This, to have different temperature measurements and make a comparison between spots. The location of thermocouples was governed by availability of suitable places, this to ensure the reproducibility of this experiment in the future. The temperature reading was performed with the thermocouples configuration given in Table 4.5. In Figure 4.10 a picture of the model with the thermocouples all placed is presented.

Channel 6 was for the Environment temperature, thus, the sensor is not shown in the model.

Channel	Spot
1	Left endwinding
2	Slot winding
3	Right endwinding
4	Model centre
5	Cage
6	Environment
7	Coil centre

Table 4.5: Picoscope Channels Configuration

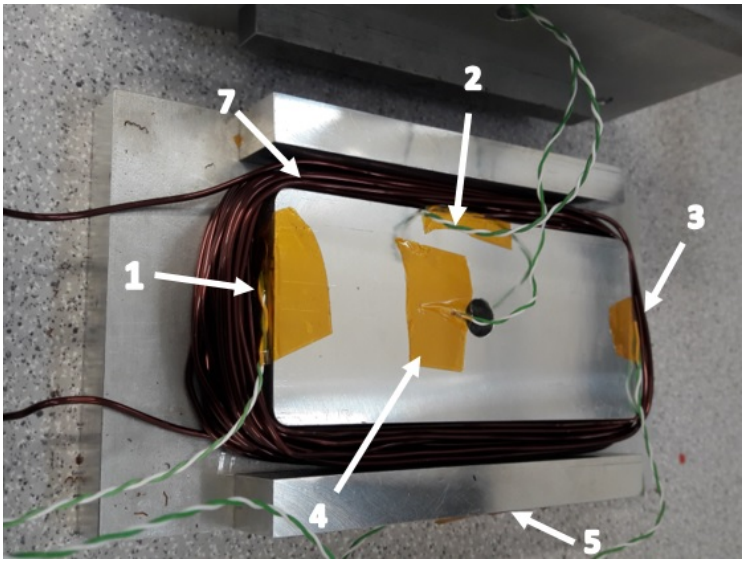

Figure 4.10: Testing Spots

After the thermocouples were correctly placed and the channels configuration in Piclog 6 was done, the system was ready to initiate with the experiment. The steps followed to initialize the power supply were:

1. Read the initial resistance of the winding

2. Properly connect the wire ends to the source terminal

3. Verify thermocouples are reading temperature

4. Supply 6 *Amps* constant current

This process was followed rigorously the same with the three systems. In Figure 4.11 the experiment being supplied is observed.

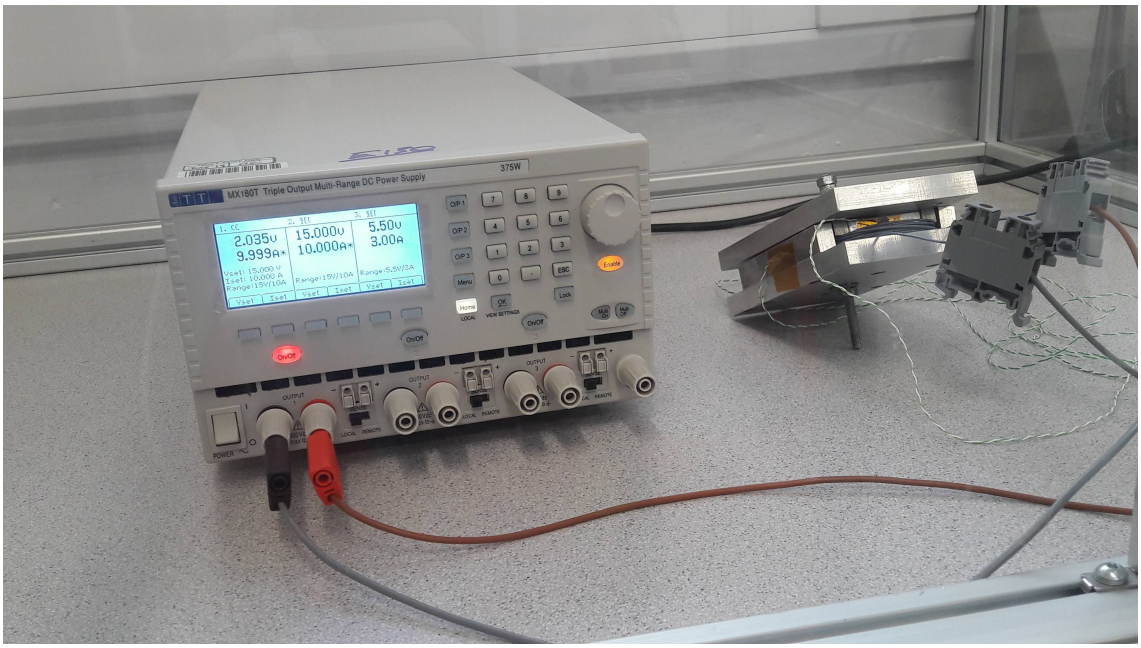

Figure 4.11: Power Supply

In figure 4.12 the configuration process of the system is summarized.

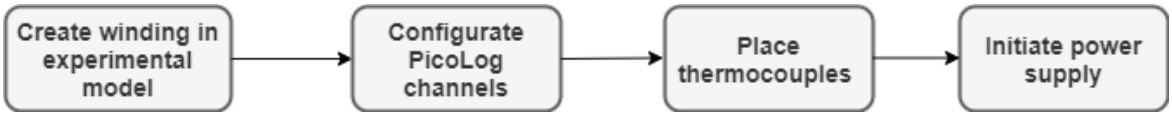

Figure 4.12: System Configuration

4.2 Experimental Thermal Test

Once the system was connected, a DC current of 6 Amperes was supplied into the winding. This power was supplied until the system thermal steady-state was attained, because, as mentioned in [18, 20], most losses arise during steady state operation. The time to get this steady state was similar in every arrangement, as

it can be observed in Figure 4.15, 4.17 and 4.19. During this period, as specified in 4.1, intervals of 15 minutes were worked to obtain the voltage reading data from the beginning until the end of the experiment for the further resistances calculations.

Through the PicoLog 6 interface, the measured temperature data was obtained and stored in the computer. Afterwards, a Matlab code was created to plot the thermal equation 3.2.3, $R = R_0[1 + \alpha(T - T_0)]$, in order obtain the resistance based on the temperature data. The same way, resistance was plotted from the voltage readings with Function 4.2.1:

$$R = \frac{V}{I} \tag{4.2.1}$$

where V stands for the voltage values obtained through the sampling process and the fixed current value. Both functions were plotted together to compare resistance values in the 3 experimental cases. The experiment process is resumed in Figure 4.13.

Figure 4.13: Thermal Test Process

4.3 Experimental Results

4.3.1 Arrangement 1. Conventional Insulated Winding Wire

In Figure 4.14 the created winding can be observed. Table 4.6 summarizes the results obtained of running this thermal experiment until the system raised the steady-state. In Figure 4.15, both resistances functions, temperature based and voltage based, are shown.

Variables	Value
Initial resistance	126.899 $m\Omega$
Final resistance	137.601 $m\Omega$
Initial temperature	21.196 $°C$
Final temperature	43.147 $°C$
Voltage rise	0.046 V
Power supply time	305 minutes

Table 4.6: Results of Arrangement 1

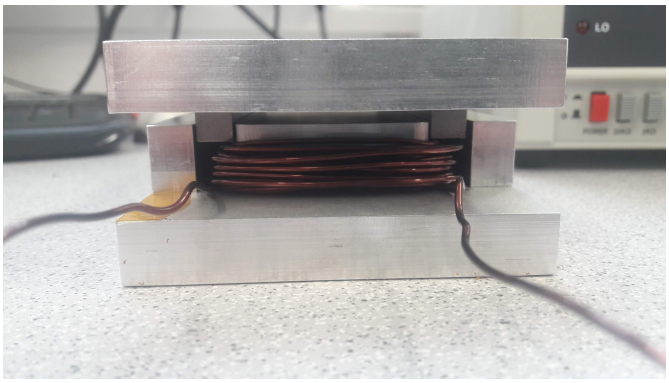

Figure 4.14: Experimental Winding

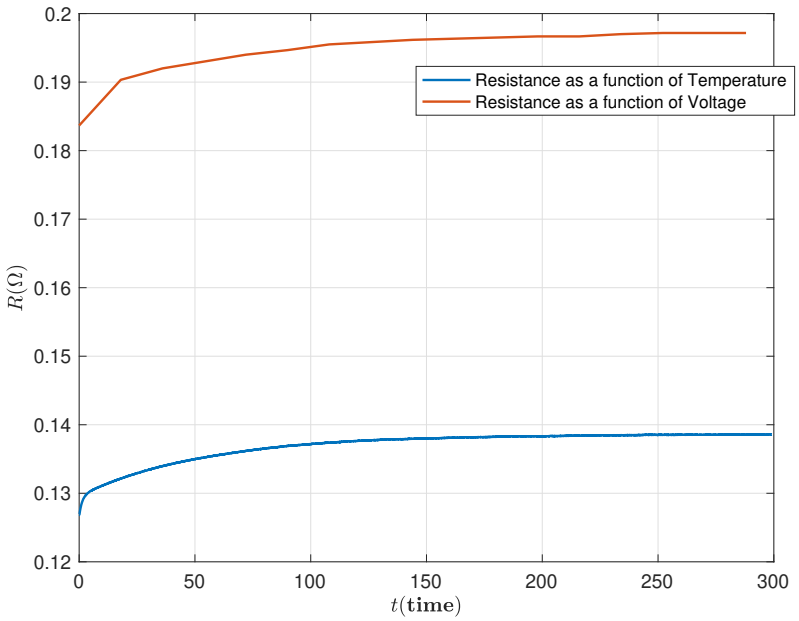

Figure 4.15: Resistance Rise with Arrangement 1

4.3.2 Arrangement 2. Conventional Insulated Winding Wire with Slot Liner

In this second arrangement, the same winding was used and a slot paper was included in the experiment, just as it is commonly made in induction motor stator winding, in order to observe the temperature behaviour. The power supply was run for 300 minutes until the system raised the thermal steady-state. The voltage was read every 15 minutes. Table 4.7 presents the results and the resistances plot is shown in Figure 4.17.

Variables	Value
Initial resistance	126.899 $m\Omega$
Final resistance	138.500 $m\Omega$
Initial temperature	18.955 $°C$
Final temperature	42.138 $°C$
Voltage rise	0.081 V
Power supply time	300 minutes

Table 4.7: Results of Arrangement 2

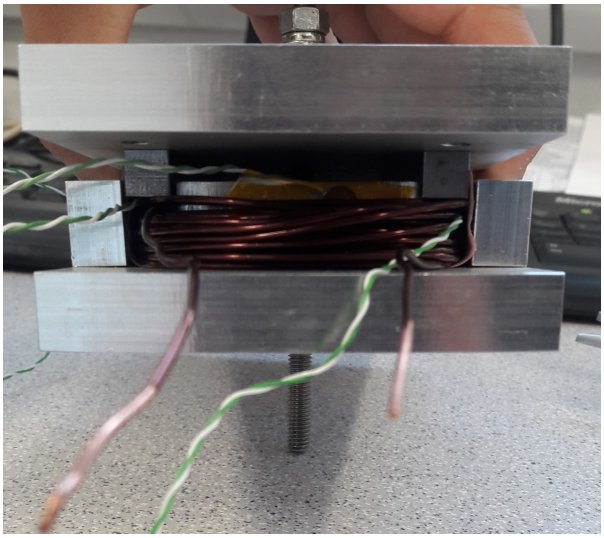

Figure 4.16: Arrangement 2

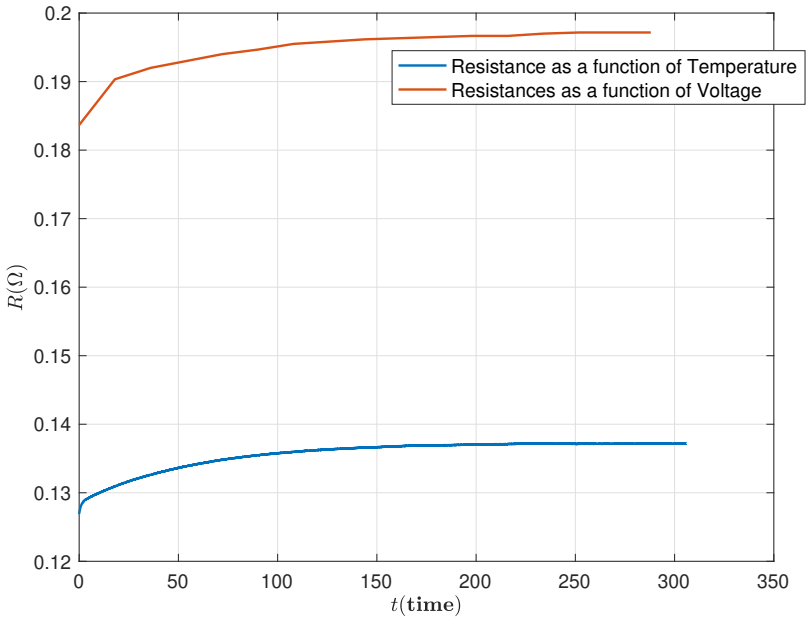

Figure 4.17: Resistance Rise with Arrangement 2

4.3.3 Arrangement 3. PEEK Insulated Winding Wire

In Figure 4.18, the winding created with PEEK insulated wire can be observed. The results of this third experiment are summarized in Table 4.8 and the resistances plot is shown in Figure 4.19.

Variables	Value
Initial resistance	137.190 $m\Omega$
Final resistance	151.150 $m\Omega$
Initial temperature	22.153 $°C$
Final temperature	48.725 $°C$
Voltage rise	0.070 V
Power supply time	320 minutes

Table 4.8: Results of Arrangement 3

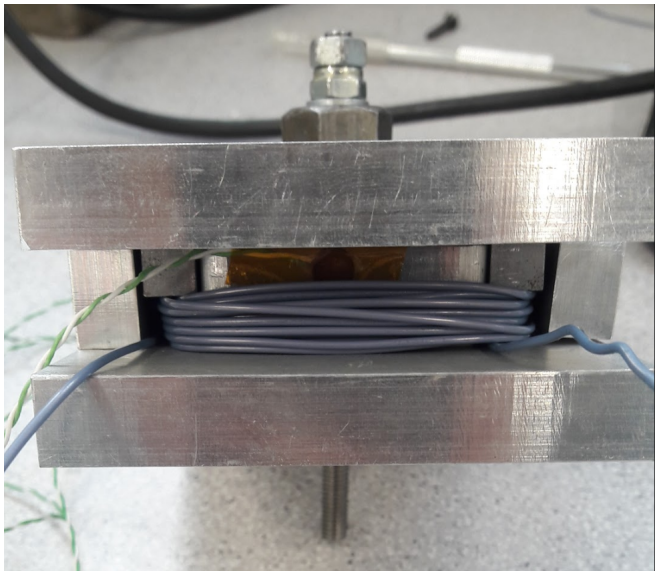

Figure 4.18: Arrangement 3

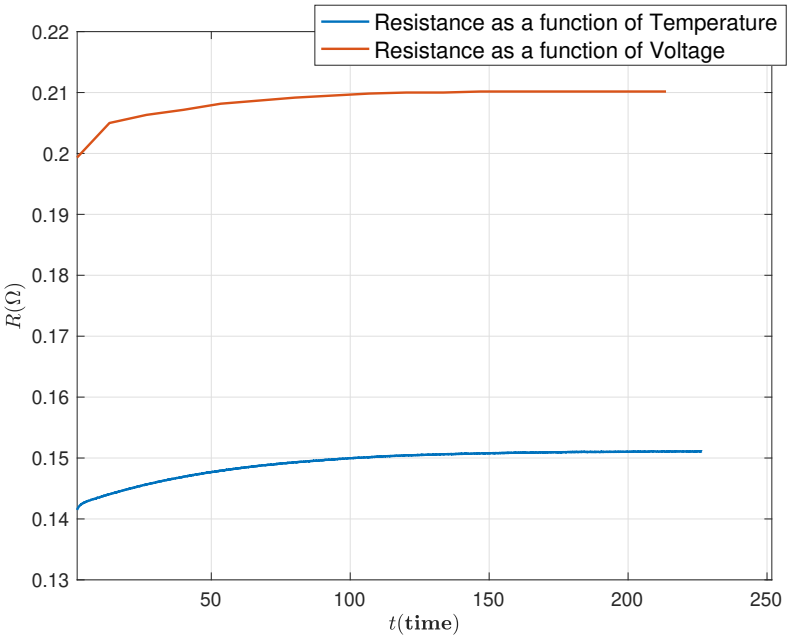

Figure 4.19: Resistance Rise with Arrangement 3

4.4 Results Analysis

As it can be observed on the graphics, the resistances obtained with PEEK insulated wire is higher. The results in resistance and temperature increment can be observed in Table 4.9.

Arrangement	Resistance increment	Temperature Increment
Copper wire	10.800 $m\Omega$	21.951 $°C$
Copper wire and slot paper	11.601 $m\Omega$	23.183 $°C$
PEEK insulated wire	13.960 $m\Omega$	26.573 $°C$

Table 4.9: Resistances and Temperature Increment Comparison

As appreciated in Figure 4.19, the PEEK experiment had a higher resistance. It is assumable that the temperature would variate in the third experiment because of the differences between the wires characteristics. Results might indicate that the PEEK thermal conductivity has not helped the winding to limit the temperature rise. Analysing the conditions of the wires, observed in Table 4.10, the diameter of the conductor material in the PEEK insulated wire is smaller that the varnish copper wire, so is the cross section.

Diameters	Value
PEEK copper wire	$1.13mm$
PEEK insulated wire	$1.25mm$
Varnish copper wire	$1.22mm$
Varnish insulated wire	$1.29mm$

Table 4.10: Wires Diameters

In Figure 4.20 the cross section of both wires can be appreciated. Table 4.11 presents the dimensions as well as the fill factor obtained with the wires in every case, stating the slot area as $60mm^2$ as presented in Chapter 4.1. In Table 4.11 it can be observed that the fill factor obtained with the varnish insulated wire is higher than the one obtained with the PEEK insulated wire, therefore, it remains essential to consider the wire differences to develop an analyse of resistances in both wires.

Wire	Cross Section	Slot Fill Factor
PEEK insulated wire	$1.0028mm^2$	50.14 %
Varnish insulated wire	$1.1689mm^2$	58.45 %

Table 4.11: Wires Cross Sections

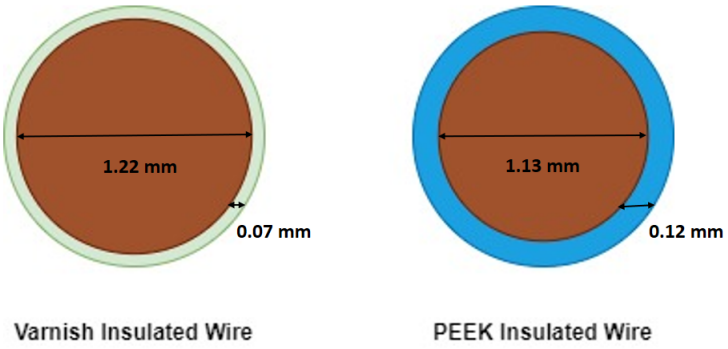

Figure 4.20: Wires Dimensions

As stated in Equation 3.2.1, $R = \frac{\rho L}{A}$, presented in Chapter 3, resistance is inversely proportional to the cross area. Resistivity ρ and length L are the same for both conductors. Thus, it could be inferred than the resistance in the PEEK Arrangement would result higher.

The resistance estimation in section 4.3 were plotted with Function 3.2.3, $R = R_0[1 + \alpha(T - T_0)]$. Nevertheless, it is essential to analyse this experiment with Function 3.2.1 as the cross section is a critical variable to consider, thus the two types of wire were evaluated. According to Function 3.2.1, resistance for varnished copper wire is obtained as shown in 4.4.2:

$$R_e = \frac{\rho L}{A_e} \tag{4.4.2}$$

where R_e is the resistance in the varnished insulated wire and A_e is the cross section of the conductor. The same way, for the PEEK insulated wire, Function 4.4.3 calculates the resistance, where R_p is the resistance and A_p stands for the corresponding cross section.

$$R_p = \frac{\rho L}{A_p} \tag{4.4.3}$$

Equation 4.4.2 could be expressed as presented in Equation 4.4.4.

$$R_e A_e = \rho L \tag{4.4.4}$$

Equation 4.4.3 can then, be expressed as follows:

$$R_p A_p = \rho L \tag{4.4.5}$$

As it can be observed, ρ and L are the same for both equations as the conductors have the same conductivity and length. Following this comparison, Equation 4.4.6 assume the following equivalence:

$$R_e A_e = R_p A_p \tag{4.4.6}$$

According to this function, R_p can be expressed as follows:

$$R_p = \frac{R_e A_e}{A_p} \tag{4.4.7}$$

Also R_e can be expressed the same way:

$$R_e = \frac{R_p A_p}{A_e} \tag{4.4.8}$$

In order to compare these equivalences with the resistance estimation obtained in Chapter 4.3, Function 4.4.7 and 4.4.8 were compared with Function 3.2.3. These are presented in Figure 4.21, comparing the resistances in the varnish insulated wire and in Figure 4.22 that compares resistance in the PEEK insulated wire.

In Figure 4.21 it can be observed that the analysed resistance resulted lower that the one estimated with temperature in the varnish instulated wire. The opposite way occurred in 4.22, where resistance after the analyse resulted higher.

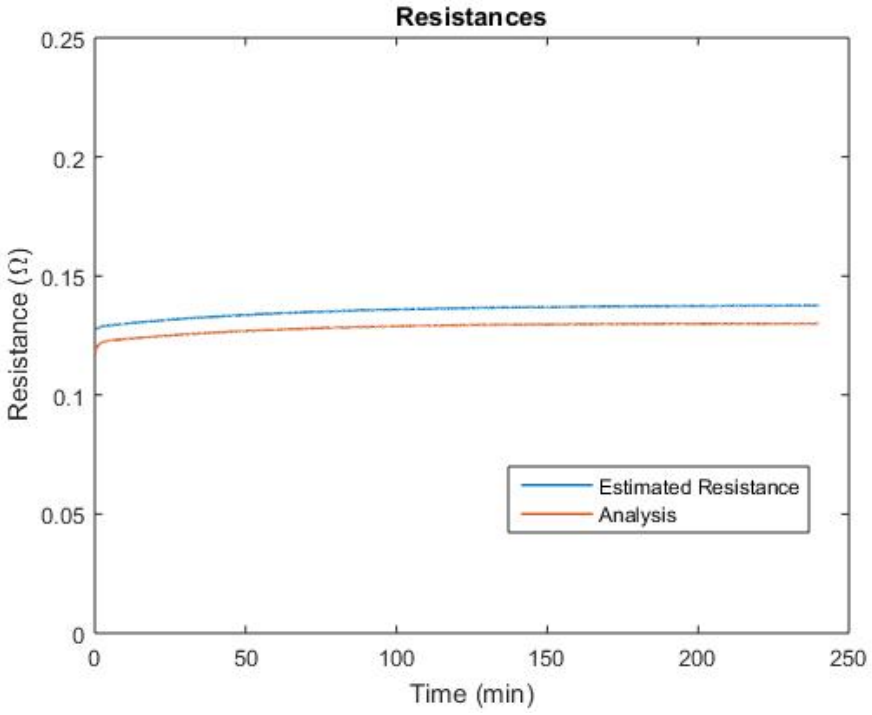

Figure 4.21: Varnish Insulated Wire Resistances Comparison

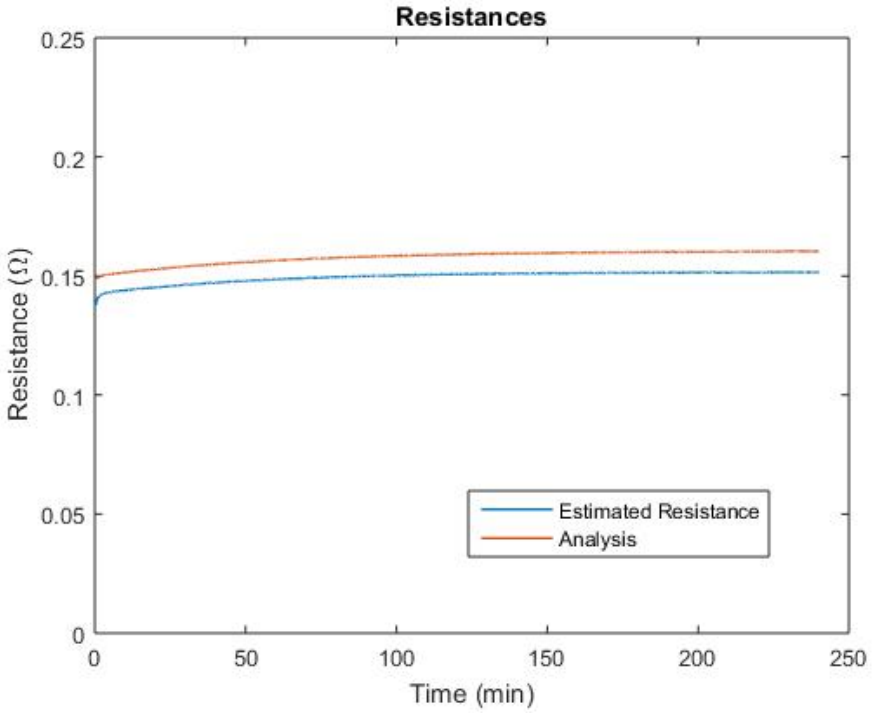

Figure 4.22: PEEK Insulated Wire Resistances Comparison

As observed in Figure 4.21 and Figure 4.22 the analysis realized based on Functions 4.4.7 and 4.4.8 presents a possible explanation of the resistance rise in the PEEK insulated wire due to the difference in the conductor cross section, which were $1.0028mm^2$ in the PEEK insulated wire and $1.1689mm^2$ in the varnish insulated wire. These analysed resistance results are close to the estimations obtained in the experiment with Equation 3.2.3. Table 4.12 present the uncertainties of the obtained values.

Case	Value
R_e	$8.2 \pm 0.6\ m\Omega$
R_p	$9.6 \pm 0.7\ m\Omega$

Table 4.12: Uncertainties

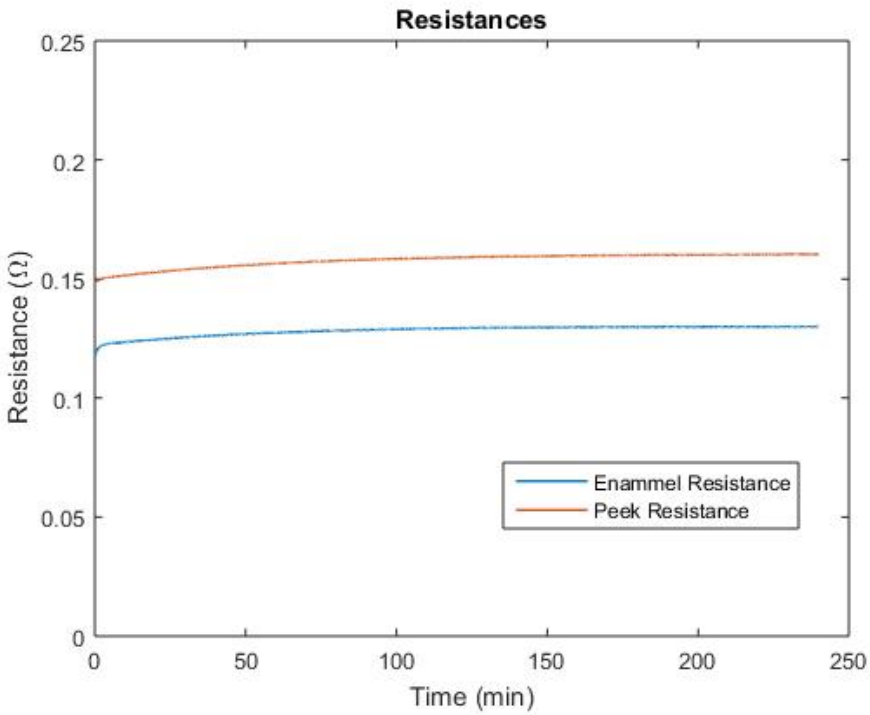

Figure 4.23: Final Analysis

To compare analysed resistances, PEEK and varnished wire resistances after the analysis were plotted together. From the data presented in Figure 4.23, it is observed that the resistance of PEEK insulated wires remains higher than the resistance in

the varnish insulated wire after considering the cross section variable of the copper wire. With this final plot presented in Figure 4.23, the analysis developed for R_e and R_p confirms the results obtained with the thermal experiments in Chapter 4.3; in this experiment resistance of PEEK insulated wire is higher than the varnish insulated wire due to the difference in the copper cross section.

Chapter 5

Conclusions

Promoting effectively a global motor market transformation, will have a strong impact on the electrical energy consumption all over the world. Energy efficiency in electric motors has several opportunities to work in order to be improved, being a big opportunity to obtain savings in both, energy and money. In this research, the implementation of a different wire insulation as an alternative to the usual enamel to decrease resistive losses was proposed and tested. The stator copper losses are in function of resistance, and resistance increases in function of temperature. With this in mind, it was inferred that with better insulation characteristics, it would be possible to decrease the losses. In this thesis, 3 different insulation arrangements were tested in order to be compared. The temperature of a stator model was measured focusing on obtaining the winding resistance. For this purpose, a constant current of $6A$ was supplied into the created winding and the temperature was measured until the steady-state was reached, variation in reaching the steady-state was affected also for the variation of the ambient temperature in the three cases. It could be observed that the time to reach thermal steady-state is close in the three arrangements due to the similarities of the systems. Once the experimental work was run, resistance from the temperature data graphics were generated and analysed to evaluate the performance of the three systems. With the obtained temperature data, the resistance has been calculated with a specified function. Experimental results have shown that resistance in the winding created with PEEK insulated wire apparently did not resulted to decrease the resistance rise.

To verify the obtained estimations, an analyse of the two wires resistances was carried out to obtain resistance with a function that considerates the wires characteristics; length, resistivity and cross sections. These resistance analysed in fuction of conductor cross section and length are close to the experimental results. Uncertainties were presented and an explanation is provided

This experimental model was created manually, there exist variables that could not be controlled as temperature and filling factor. It was not the most suitable way to create this winding, but it was decided to create it this way because of the differences between existing materials. Experimental results have shown that resistance in the winding created with PEEK insulated wire, did not decrease the resistance rise, but, after the analyse, it can be conclude that this is due to the copper wire cross section which was smaller than in the varnish insulated wire. Thus, it is highly recommended to repeat this experiment with the same materials characteristics in order to obtain a more precise resistance rise estimation.

5.1 Future Work

The experiments developed in this thesis play and important role for further research in windings insulation to be done. The thermal experiments may represent a base for different kind of work, fill factor could not be worked in this project due to the differences in the winding wires. Nevertheless it would result interesting to work with the slot filling factors and test different percentages of them. Packing patterns and also wire geometry can be worked in order to achieve a higher fill factor.

It would be essential to repeat the experiment with higher quality winding, obtaining copper wires with the same cross section also with the two different insulation in the same width and repeat the experiment with the same electric fill factor in the stator slots to make a more accurate materials performance comparison. The experiments can also work the infill technique, implementing resins to fill the space in the slot that cannot be occupied with wire. Furthermore, it is necessary to keep the initial temperature under control to prevent variation in the experiment. An idea for it is to repeat the experiment isolated to eliminate the ambient temperature

change than was no consider on this first experiment. It could also be an option to experiment with bigger size of wires.

The experimental work can be developed applying this time an AC current, as this is the way induction motors works. The experiment could also be developed for different types of motors or generators to evaluate the development and feasibility of the proposed material. In addition, economical areas could be evaluated as new materials and different costs are implicit in this experiment. Life-cycle costs, pay-back periods, cost of ownership, cost of energy and savings in electrical machines could be calculated in order to complement this research.

Bibliography

[1] J. Yu, T. Zhang, and J. Qian, *Electrical Motor Products: International Energy-efficiency Standards and Testing Methods*. Elsevier, 2011.

[2] A. T. d. Almeida, F. J. T. E. Ferreira, and G. Baoming, "Beyond induction motors—technology trends to move up efficiency," *IEEE Transactions on Industry Applications*, vol. 50, no. 3, pp. 2103–2114, 2014.

[3] A. Castagnini, M. L. Maggi, P. S. Termini, and M. Vetuschi, "Efficiency and regulations: Pm-assisted synchronous reluctance motors as a sustainable industrial solution," in *2015 IEEE Workshop on Electrical Machines Design, Control and Diagnosis (WEMDCD)*, pp. 72–78.

[4] G. Wang and S. Park, "Improved estimation of induction motor circuit parameters with published motor performance data," in *2014 Sixth Annual IEEE Green Technologies Conference*, pp. 25–28.

[5] A. T. d. Almeida, F. J. T. E. Ferreira, J. A. C. Fong, and C. U. Brunner, "Electric motor standards, ecodesign and global market transformation," in *2008 IEEE/IAS Industrial and Commercial Power Systems Technical Conference*, pp. 1–9.

[6] D. Liang and V. Zhou, "Recent market and technical trends in copper rotors for high-efficiency induction motors," in *2018 International Power Electronics Conference (IPEC-Niigata 2018 -ECCE Asia)*, pp. 1943–1948.

[7] J. Pyrhonen, T. Jokinen, and V. Hrabovcova, *Design of rotating electrical machines*. John Wiley and Sons, 2013.

[8] D. H. Kang, E. Figueiredo, J. Kruckel, S. C. A. Arkkio, S. Ekram, T. Obata, J. H. Kim, J. Petro, and J. Pyrhonen, "Technological feasibility studies for supper and ultra premium efficient motors," 2018.

[9] F. J. T. E. Ferreira, G. Baoming, and A. T. d. Almeida, "Reliability and operation of high-efficiency induction motors," *IEEE Transactions on Industry Applications*, vol. 52, no. 6, pp. 4628–4637, 2016.

[10] S. Baldwin, *Energy-Efficient Electric Motor Drive Systems*, p. 960. 1989.

[11] IEC, "Rotating electrical machines part 30-1: Efficiency classes of line operated ac motors," 2014.

[12] C. Y. Liu, Y. W. Hsieh, T. J. Sun, J. W. Zeng, A. B. Wang, N. T. Lee, S. W. Chau, W. C. Wei, B. H. Liu, and R. C. Luo, "Design and test of additive manufacturing for coating thermoplastic peek material," in *2016 IEEE International Conference on Industrial Technology (ICIT)*, pp. 1158–1162.

[13] E. H. Werninck, *Electric motor handbook*. London: London : McGraw-Hill, 1978.

[14] A. Hughes and B. Drury, *Electric Motors and Drives: Fundamentals, Types and Applications*. Elsevier Science, 2013.

[15] C. Li, D. Xu, and G. Wang, "High efficiency remanufacturing of induction motors with interior permanent-magnet rotors and synchronous-reluctance rotors," in *2017 IEEE Transportation Electrification Conference and Expo, Asia-Pacific (ITEC Asia-Pacific)*, pp. 1–6.

[16] T. Wildi, *Electrical machines, drives, and power systems*. Upper Saddle River, N.J. London: Upper Saddle River, N.J. London : Pearson/Prentice Hall, 6th ed., international ed. ed., 2006.

[17] P. Preecha and J. Dejvises, "The power losses calculation technique of electrical machines using the heat transfer theory," in *2007 International Power Engineering Conference (IPEC 2007)*, pp. 297–301, 2007.

[18] O. Badran, H. Sarhan, and B. Alomour, *Thermal performance analysis of induction motor*, vol. 30. 2012.

[19] F. J. T. E. Ferreira, A. M. Silva, V. P. B. Aguiar, R. S. T. Pontes, E. C. Quispe, and A. T. d. Almeida, "Overview of retrofitting options in induction motors to improve their efficiency and reliability," in *2018 IEEE International Conference on Environment and Electrical Engineering and 2018 IEEE Industrial and Commercial Power Systems Europe (EEEIC / ICPS Europe)*, pp. 1–12.

[20] S. Sujitjorn and K. L. Areerak, "Numerical approach to loss minimization in an induction motor," *Applied Energy*, vol. 79, no. 1, pp. 87–96, 2004.

[21] K. S. Kim, H. J. Kim, and J. P. Hong, "Thermal equivalent circuit network for outer rotor type motors," in *7th IET International Conference on Power Electronics, Machines and Drives (PEMD 2014)*, pp. 1–4, 2014.

[22] M. Abbaspour, N. Sargolzaei, and A. Namadchian, "Estimating electrical parameters of the induction motor by measuring the components temperatures," *Majlesi Journal of Electrical Engineering*, vol. 08, pp. 79–85, 2014.

[23] H. Dalvand and M. Zare, "Techno-economic evaluation of energy efficiency measures in iranian industrial 3-phase electric motors," in *2006 IEEE International Power and Energy Conference*, pp. 1–5.

[24] M. Popescu, D. G. Dorrell, L. Alberti, N. Bianchi, D. A. Staton, and D. Hawkins, "Thermal analysis of duplex 3-phase induction motor under fault operating conditions," in *2012 XXth International Conference on Electrical Machines*, pp. 1875–1881.

[25] A. Bousbaine, M. McCormick, and W. Low, "In-situ determination of thermal coefficients for electrical machines," *IEEE Transactions on Energy Conversion*, vol. 10, no. 3, pp. 385–391, 1995.

[26] R. E. West, F. Kreith, and C. Chemical Rubber, *CRC handbook on energy efficiency*. Boca Raton, FL: Boca Raton, FL : CRC Press, 1996.

[27] R. Boteler and J. Malinowski, "Review of upcoming changes to global motor efficiency regulations," in *Conference Record of 2009 Annual Pulp and Paper Industry Technical Conference*, pp. 26–30.

[28] A. T. D. Almeida, F. J. T. E. Ferreira, and A. Q. Duarte, "Technical and economical considerations on super high-efficiency three-phase motors," *IEEE Transactions on Industry Applications*, vol. 50, no. 2, pp. 1274–1285, 2014.

[29] ABB, "Powering the world economy. Is there a better way to use electricity," 2015.

[30] S. Stoft, *Power system economics : designing markets for electricity*. New York: New York : Wiley-Academy, 2001.

[31] V. Goman, V. Prakht, V. Kazakbaev, and V. Dmitrievskii, "Comparative study of induction motors of ie2, ie3 and ie4 efficiency classes in pump applications taking into account co2 emission intensity," *Applied Sciences*, vol. 10, no. 23, p. 8536, 2020.

[32] Y. Wada, N. Watanabe, M. Nakamura, and I. Hirotsuka, "A study on the characteristic of concentrated-winding induction motor," in *2018 21st International Conference on Electrical Machines and Systems (ICEMS)*, pp. 607–611.

[33] T. Jung, C. Yun, H. Cha, M. Chae, and H. Kim, "Improved design for driving characteristics in single phase induction motor with concentrated winding," in *2007 IEEE Power Electronics Specialists Conference*, pp. 2418–2422.

[34] L. Siesing, A. Reinap, and M. Andersson, "Thermal properties on high fill factor electrical windings: Infiltrated vs non infiltrated," in *2014 International Conference on Electrical Machines (ICEM)*, pp. 2218–2223.

[35] M. Galea, C. Gerada, T. Raminosoa, and P. Wheeler, "A thermal improvement technique for the phase windings of electrical machines," *IEEE Transactions on Industry Applications*, vol. 48, no. 1, pp. 79–87, 2012.

[36] D. Jaksic, ""getting rid of the air", or how to maximize winding fill factor (id 81)," in *2011 1st International Electric Drives Production Conference*, pp. 84–87.

[37] S. Makita, Y. Ito, T. Aoyama, and S. Doki, "The proposal of a new motor which has a high winding factor and a high slot fill factor," in *2014 International Power Electronics Conference (IPEC-Hiroshima 2014 - ECCE ASIA)*, pp. 3823–3827.

[38] A. O. D. Tommaso, F. Genduso, R. Miceli, and C. Nevoloso, "Fast procedure for the calculation of maximum slot filling factors in electrical machines," in *2017 Twelfth International Conference on Ecological Vehicles and Renewable Energies (EVER)*, pp. 1–8.

[39] P. Herrmann, P. Stenzel, U. Vögele, and C. Endisch, "Optimization algorithms for maximizing the slot filling factor of technically feasible slot geometries and winding layouts," in *2016 6th International Electric Drives Production Conference (EDPC)*, pp. 149–155.

[40] L. Sang-Bin, T. G. Habetler, R. G. Harley, and D. J. Gritter, "An evaluation of model-based stator resistance estimation for induction motor stator winding temperature monitoring," *IEEE Transactions on Energy Conversion*, vol. 17, no. 1, pp. 7–15, 2002.

[41] P. Mynarek and M. Kowol, "Thermal analysis of three-phase induction motor using circuit models," in *Electrodynamic and Mechatronic Systems*, pp. 119–122, 2011.

[42] M. Sabaghi, H. Farahani, H. Hafezi, P. Kiani, and A. Jalilian, "Stator winding resistance estimation for temperature monitoring of induction motor under unbalance supplying by dc injection method," pp. 217–222, 10 2007.

[43] G. Stone, E. Boulter, I. Culbert, and H. Dhirani, *Electrical Insulation for Rotating Machines: Design, Evaluation, Aging, Testing, and Repair*. Wiley, 2004.

[44] X.-j. Li, J. Yang, B.-q. Yan, and X. Zheng, "Insulated cable temperature calculation and numerical simulation," *MATEC Web of Conferences*, vol. 175, p. 03014, 2018.

[45] H. Weili, H. Weijian, and L. Lin, "Estimation of stator resistance and temperature measurement in induction motor using wavelet network," in *2007 Chinese Control Conference*, pp. 203–207.

[46] F. J. T. E. Ferreira, B. Leprettre, and A. T. d. Almeida, "Comparison of protection requirements in ie2-, ie3-, and ie4-class motors," *IEEE Transactions on Industry Applications*, vol. 52, no. 4, pp. 3603–3610, 2016.

[47] International Electrotechnical Commission, "Electrical insulation-thermal evaluation and designation," 2007.

[48] J. K. Fink, *Chapter 6 - Poly(aryl ether ketone)s*, pp. 153–175. William Andrew Publishing, 2014.

[49] Zeus, "Peek Insulated wire Engineered For Challenging Environments ," 2017.

[50] N. F. Howard Perose, "Impact on low voltage motor performance with zeus peek insulation product," report, ZEUS, 2016.

[51] Y. Çengel, *Heat Transfer: A Practical Approach*. McGraw-Hill, 2003.

[52] Young and Freedman, *University Physics with Modern Physics*. Pearson Education, 2008.